On the Design of Multi-Rate Tracking Controllers: Application to Rotorcraft Guidance and Control

Duarte Antunes[1], Carlos Silvestre[1,*] and Rita Cunha[1]

[1] *Instituto Superior Técnico, Institute for Systems and Robotics, 1049-001 Lisbon, Portugal Av. Rovisco Pais*

SUMMARY

This paper presents a new methodology for the design and implementation of gain-scheduled controllers for multi-rate systems. The proposed methodology provides a natural way to address the integrated guidance and control problem for autonomous vehicles when the outputs are sampled at different instants of time. A controller structure is first proposed for the regulation of non-square multi-rate systems with more measured outputs than inputs. Based on this structure, an implementation for a gain-scheduled controller is obtained that satisfies an important property known as the linearization property. The implementation resembles the velocity implementation for single-rate systems. The method is then applied to the problem of steering an autonomous rotorcraft along a predefined trajectory defined in terms of space and time coordinates. By considering a convenient error vector to describe the vehicle's dynamics the trajectory tracking problem is reduced to that of regulating the error variables to zero. Due to the periodic multi-rate nature of the onboard sensor suite, the controller synthesis is dealt with under the scope of linear periodic systems theory. Simulation results obtained with a full non-linear rotorcraft dynamic model are presented and discussed.

KEY WORDS: *multi-rate control*; *gain-scheduling control*; *output regulation*; *guidance and control*

1. INTRODUCTION

Over the last few decades there has been a surge of interest in the development of efficient and reliable guidance and control algorithms for unmanned vehicles. An endless number of applications are reported in the literature, ranging from underwater geological surveillance [14] to spacecraft missions [19]. Increasing advances in sensor technology call for the development and design of control systems capable of taking full advantage of the sensors characteristics. Moreover, the designer is often faced with challenging control problems due to the choice of cost-effective sensor solutions.

*Correspondence to: Instituto Superior Técnico, Institute for Systems and Robotics, 1049-001 Lisbon, Portugal Av. Rovisco Pais 1

Contract/grant sponsor: Fundação para a Ciência e a Tecnologia (ISR/IST pluriannual funding) through the POS_Conhecimento Program that includes FEDER funds and by the ALTICOPTER project; contract/grant number: SFRH/BD/24632/2005

Traditionally, the guidance and control problem for autonomous vehicles involves the design of an inner and an outer loop [18]. The inner loop is designed to stabilize the vehicle dynamics and usually requires a high sampling rate, whereas the outer loop design relies essentially on the vehicle's kinematic model, converting tracking errors into inner loop commands, and is amenable to a lower sampling rate. As explained in [17], since the two systems, kinematics and dynamics, are effectively coupled, stability and adequate performance of the combined systems are not guaranteed. An interesting feature of this technique is that, since the kinematic variables are commonly available at lower rates (consider for example the case of a GPS receiver), the design of the different loops at different rates often handles naturally the multi-rate characteristic of the sensors.

Another line of work, presented in [6], [9], [17] proposes and integrated solution for the guidance and control problem. This solution amounts to applying a conveniently defined path-dependent transformation to the vehicle's equations of motion, which involves both kinematic and dynamic variables of the vehicle. In this new space, referred to as error-space, the problems of trajectory tracking or path-following reduce to the problem of driving this newly-defined error to zero. The family of error transformations presented in [6], [9], [17] have the notable property of guaranteeing that the linearization of the error dynamics is time-invariant along trimming trajectories, which comprise arbitrary straight lines and z-aligned helices. Since the vehicle's dynamic behavior changes considerably throughout its flight envelope, gain-scheduling control laws, which have become a standard solution in flight control systems, are typically used. In this setting, the multi-rate characteristics of the sensors have been traditionally handled by the navigation system design [14] without guaranteeing the performance (or even the stability) of the overall closed loop system, although the problem can be formulated as a control design problem.

This paper follows the line of work reported in [6], [9], [17], adopting the integrated guidance and control approach and proposes a novel method to take into account the multi-rate characteristics of the sensors in the controller design. To this effect, theoretical results are first derived which make use of the existing background for multi-rate systems and gain-scheduling theory. The theory for multi-rate systems is intimately related with the theory of periodically time-varying systems. See, for example, [15] and the references therein for early work on the subject and [13] for more recent developments. Noteworthy is the bulk of work in this field by Bittanti, Colaneri and co-workers. With particular interest to the present paper are the definitions of stabilizability and detectability for periodic systems [1], and the solutions of the problems of regulation for square multi-rate systems [5], output stabilization for periodic systems [3], and LQG optimal control for multi-rate systems [4]. In the field of gain-scheduling an excellent survey can be found in [16]. The commonly adopted method for the development of gain-scheduled controllers, which is also followed in the current paper, involves the following steps:

1. Obtain a family of parameter dependent linear models, usually by Jacobian linearization of the plant about a finite number of representative operating points characterized by parameter values. The parameters correspond to fixed values of scheduling variables, which are functions of internal state variables and exogenous signals.
2. Design a family of linear controllers for the family of parameter dependent linear models. If a finite set of linearized plant models is available from the first step, then linear controllers are designed for each linear model, corresponding to a fixed parameter

value, and their coefficients are interpolated. Typically the interpolation is such that the controllers coefficients depend continuously on the parameters.
3. Implement the gain-scheduled controller on the nonlinear plant. The controller coefficients (gains) computed for time-frozen parameters are changed on-line according to the current value of the scheduling variables.
4. Perform extensive simulations for the resulting control system to access its performance characteristics.

Since the controllers are designed for time-frozen parameters and when implemented the parameters are allowed to vary, the linearization of the nonlinear gain-scheduled controller about a given equilibrium point does not in general match the designed time-frozen linear controller. This mismatch is commonly known as the hidden coupling [16] and might lead to performance degradation or even instability. Therefore, for a correct implementation of the controllers, the following property is required to hold:

Linearization property: At each equilibrium point, the nonlinear gain-scheduled controller must linearize to the linear controller designed for that equilibrium.

A technique known as the velocity implementation, presented in [10], [11] and discussed in [12], [16] which is related with the work presented herein, provides a simple solution for the implementation of controllers with integral action that satisfies the linearization property.

Based on the foundations of gain-scheduling and multi-rate control theory and motivated by the problem at hand, the contributions of this paper are two fold: i) a new structure is proposed for the regulation of non-square multi-rate systems with more outputs than inputs and, based on this structure, ii) a straightforward method is obtained for the implementation of gain-scheduled controllers for multi-rate systems that satisfy the linearization property. Using these results, and casting the integrated guidance and control problem as a regulation problem, we are able to solve in a systematic manner the guidance and control problem for autonomous vehicles equipped with multi-rate sensor suite. An application of this methodology is presented which tackles the trajectory tracking problem of steering an autonomous rotorcraft along a pre-defined trajectory. The synthesis of linear controllers, one of the stages in the design of the gain-scheduled controller, makes use of the $\mathcal{H}_2$ control synthesis framework for periodic systems. The performance of the resulting non-linear multi-rate guidance and control law is compared to that obtained with a standard single-rate compensator designed using equivalent weighting matrices in the $\mathcal{H}_2$ controller design problem.

The remainder of the paper is organized as follows. First we develop a theoretical framework for the design of multi-rate gain scheduled controls valid for a wide class of non-linear systems. Section 2 describes the problem formulation and Sections 3 and 4 present the main results: the regulator structure and gain-scheduling implementation, respectively. In Section 5 we apply the proposed methodology to the design of an integrated guidance and control system that addresses the trajectory tracking problem for a small-scale rotorcraft, and evaluate the performance of the resulting nonlinear feedback system in simulation. Section 6 presents some concluding remarks.

1.1. Notation

The space of n-dimensional continuous-time signals, $x(t) : \mathbb{R}^+ \mapsto \mathbb{R}^n$, is denoted by $\mathcal{L}(\mathbb{R}^+, \mathbb{R}^n)$ or simply by $\mathcal{L}(\mathbb{R}^+)$ and the space of n-dimensional discrete-time signals, $x_k : \mathbb{Z}^+ \mapsto \mathbb{R}^n$, is denoted by $l(\mathbb{Z}^+, \mathbb{R}^n)$ or simply by $l(\mathbb{Z}^+)$. The notation $\text{diag}([a_1 \ a_2 \ \dots \ a_n])$ indicates a block diagonal matrix where the entries a_i can be either scalar or matrices. Whenever the matrices dimensions are clear, identity and zero matrices are denoted by I and 0. Otherwise the dimensions are explicit indicated as in $I_{3\times3}$, $0_{3\times2}$. A vector of n ones is denoted by $\mathbf{1_n} = [1 \ 1 \ \dots \ 1]^T$. For dimensionally compatible matrices A and B, we define $(A, B) := [A^T \ B^T]^T$. Further notation will be introduced when necessary.

2. PROBLEM FORMULATION

Consider the nonlinear system

$$G = \begin{cases} \dot{x}(t) = f(x(t), u(t), w(t)) \\ y(t) = h(x(t), w(t)) \\ z(t) = g(x(t), u(t), w(t)) \end{cases} \tag{1}$$

where $x(t) \in \mathbb{R}^n$ is the state and $u(t) \in \mathbb{R}^m$ is the control input. The vector $w(t) = [r(t)^T \ d(t)^T]^T \in \mathbb{R}^{n_w}$ is a vector of exogenous signals where $r(t)$ represents references to be tracked and $d(t)$ represents both external disturbances and measurement noise. The vector $y(t) = [y_m(t)^T \, y_r(t)^T]^T = [h_m(x(t), w(t))^T \, h_r(x(t), w(t))^T]^T \in \mathbb{R}^p$ contains a vector of measured outputs $y_m(t) \in \mathbb{R}^{n_{y_m}}$ and a vector of reference tracking outputs $y_r(t) \in \mathbb{R}^{n_{y_r}}$, which we assume to have the same dimensions as the control input, $n_{y_r} = m$. This vector is required to track the reference $r(t)$ with zero steady-state error, i.e, the vector $e(t)$ defined as

$$e(t) = y_r(t) - r(t)$$

must satisfy $e(t) = 0$ at steady-state. Some of the components of $y_r(t)$ may be included in $y_m(t)$ as well. Finally, the vector $z(t) \in \mathbb{R}^{n_z}$ is a performance output. We assume that f and g are continuously differentiable functions.

2.1. Linearization family

We assume that there exists a family of equilibrium points for G of the form

$$\Sigma = \{(x_0, u_0, w_0) : f(x_0, u_0, w_0) = 0, \ \ y_{r0} = h_r(x_0, w_0) = r_0, \ \ (x_0, u_0, w_0) \in \Omega \subset \mathbb{R}^{n+m+n_w}\} \tag{2}$$

which can be parameterized by a vector $\alpha_0 \in \Xi \subset \mathbb{R}^s$, such that

$$\Sigma = \{(x_0, u_0, w_0) = a(\alpha_0), \alpha_0 \in \Xi\}$$

where a is a continuously differentiable function. In the vector $w_0(\alpha_0) = [r_0(\alpha_0) \ d_0(\alpha_0)]$ we set $d_0(\alpha_0) = 0$ since the exogenous input d is not known in advance. We further assume that there exists a continuously differentiable function v such that $\alpha_0 = v(y_0, w_0)$. By applying the function v to the measured values of y and w, we obtain the variable

$$\alpha = v(y, w) \tag{3}$$

which is usually referred to as the scheduling variable.

Linearizing the nonlinear system G about each point in the equilibrium manifold Σ, parameterized by α_0, yields the family of linear systems

$$G_l(\alpha_0) = \begin{bmatrix} \dot{x_\delta}(t) \\ z_\delta(t) \\ y_\delta(t) \end{bmatrix} = \begin{bmatrix} A(\alpha_0) & B_1(\alpha_0) & B_2(\alpha_0) \\ C_1(\alpha_0) & D_{11}(\alpha_0) & D_{12}(\alpha_0) \\ C_2(\alpha_0) & D_{21}(\alpha_0) & 0 \end{bmatrix} \begin{bmatrix} x_\delta(t) \\ w_\delta(t) \\ u_\delta(t) \end{bmatrix} \tag{4}$$

where, for example, $A(\alpha_0) = \frac{\partial f}{\partial x}(a(\alpha_0))$ and $x_\delta(t) = x(t) - x_0$.

2.2. Multi-rate sensors and actuators

We consider that the sample and hold devices that interface the discrete-time controller and the continuous-time plant operate at different rates. The setup is shown in Figure 1, where the generic discrete-time controller is denoted by K.

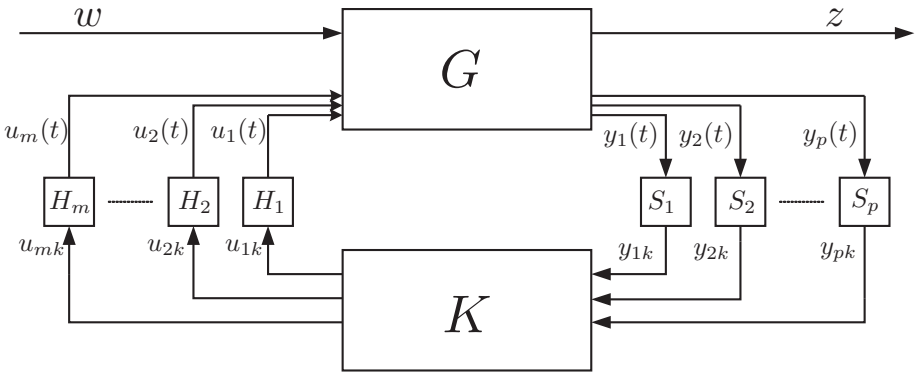

Figure 1. Multi-rate setup

Associated with each sampler S_i there is a sequence of sampling times $\{\sigma_1^i, \sigma_2^i, ..\}$ that satisfies $0 < \sigma_j^i < \sigma_{j+1}^i$. Similarly, associated with each holder H_i there is a sequence of sampling times $\{\tau_1^i, \tau_2^i, ..\}$ that satisfies $0 < \tau_j^i < \tau_{j+1}^i$. We assume that the sample and hold operations are periodic and that their periods are related by rational numbers. Thus we can define a sequence of equally spaced time instants $\{t_0, t_1, ...\}$, $t_{k+1} - t_k = t_s, k \in \mathbb{Z}^+$, such that for every sampling time σ_j^i and hold time τ_j^i there exists a k_1 and a k_2 for which $\sigma_j^i = t_{k_1}$ and $\tau_j^i = t_{k_2}$.

Each mapping $S_i : y_i(t) \in \mathcal{L}(\mathbb{R}^+) \to y_{ik} \in l(\mathbb{Z}^+)$ is given by

$$(S_i y_i)_k = g_i(k) y_i(t_k) = y_{ik}, \quad g_i(k) = \begin{cases} 1 & \text{if } \sigma_j^i = t_k \text{ for some } j \\ 0 & \text{otherwise} \end{cases}$$

meaning that the output of the sampler S_i is zero if channel i is not sampled at time t_k, and

each mapping $H_i : u_{ik} \in l(\mathbb{Z}^+) \to u_i(t) \in \mathcal{L}(\mathbb{R}^+)$ is given by

$$\begin{aligned}
&\xi_{ik+1} = (1 - r_i(k))\xi_{ik} + r_i(k)u_{ik}, \quad \xi_{i0} = 0 \\
&\tilde{u}_{ik} = (1 - r_i(k))\xi_{ik} + r_i(k)u_{ik} \qquad r_i(k) = \begin{cases} 1 & \text{if } \tau_j^i = t_k \text{ for some } j \\ 0 & \text{otherwise} \end{cases} \\
&u_i(t) = \tilde{u}_{ik} \qquad t \in [t_k, t_{k+1})
\end{aligned}$$

Defining the matrices

$$\Gamma_k = \text{diag}(g_1(k), ..., g_p(k))$$

and

$$\Omega_k = \text{diag}(r_1(k), ..., r_m(k))$$

the multi-rate sample and hold operations can be written in compact form as

$$\begin{aligned}
S: \quad & y(t) \in \mathcal{L}(\mathbb{R}^+) \to y_k \in l(\mathbb{Z}^+) \\
& y_k = \Gamma_k y(t_k) \\
H: \quad & u_k \in l(\mathbb{Z}^+) \to u(t) \in \mathcal{L}(\mathbb{R}^+) \\
& \xi_{k+1} = (I - \Omega_k)\xi_k + \Omega_k u_k \quad \xi_0 = 0 \\
& \tilde{u}_k = (I - \Omega_k)\xi_k + \Omega_k u_k \\
& u(t) = \tilde{u}_k \qquad t \in [t_k, t_{k+1})
\end{aligned} \tag{5}$$

where due to the periodic nature of the sample and hold devices, for some positive integer h which denotes the period, we have

$$\Gamma_k = \Gamma_{k+h} \qquad \Omega_k = \Omega_{k+h}.$$

This set of h-periodic matrices completely characterize the multi-rate setup.

The operators $S : \mathcal{L}(\mathbb{R}^+) \to l(\mathbb{Z}^+)$ and $H : l(\mathbb{Z}^+) \to \mathcal{L}(\mathbb{R}^+)$ can be decomposed into $S = \Gamma_d S_{t_s}$ and $H = H_{t_s}\Omega_d$, with

$$\begin{aligned}
&\Omega_d : u_k \in l(\mathbb{Z}^+) \to \tilde{u}_k \in l(\mathbb{Z}^+) \\
&\quad \xi_{k+1} = (I - \Omega_k)\xi_k + \Omega_k u_k \quad \xi_0 = 0 \\
&\quad \tilde{u}_k = (I - \Omega_k)\xi_k + \Omega_k u_k
\end{aligned} \qquad \begin{aligned}
&H_{t_s} : \tilde{u}_k \in l(\mathbb{Z}^+) \to u(t) \in \mathcal{L}(\mathbb{R}^+) \\
&\quad u(t) = \tilde{u}_k \quad t \in [t_k,\, t_{k+1})
\end{aligned}$$

$$\begin{aligned}
&S_{t_s} : y(t) \in \mathcal{L}(\mathbb{R}^+) \to \tilde{y}_k \in l(\mathbb{Z}^+) \\
&\quad \tilde{y}_k = \begin{bmatrix} \tilde{y}_{mk} \\ \tilde{y}_{rk} \end{bmatrix} = y(t_k)
\end{aligned} \qquad \begin{aligned}
&\Gamma_d : \tilde{y}_k \in l(\mathbb{Z}^+) \to y_k \in l(\mathbb{Z}^+) \\
&\quad y_k = \Gamma_k \tilde{y}_k = \begin{bmatrix} \Gamma_{mk} & 0 \\ 0 & \Gamma_{rk} \end{bmatrix} \begin{bmatrix} \tilde{y}_{mk} \\ \tilde{y}_{rk} \end{bmatrix}
\end{aligned}$$

where $\Gamma_k = \begin{bmatrix} \Gamma_{mk} & 0 \\ 0 & \Gamma_{rk} \end{bmatrix}$ has been partitioned according to the output decomposition $y^T = [y_m^T \; y_r^T]$.

The following definitions will also be useful. Given the set of matrices $\Gamma_k \;, k = 0, .., h-1$, we define Γ as

$$\bar{\Gamma} = \text{diag}([\Gamma_0 \;\; \Gamma_1 \;\; \dots \Gamma_{h-1}]) \tag{6}$$

which is of the form $\bar{\Gamma} = \text{diag}([\gamma_1 \;\; \gamma_2 \;\; \dots \;\; \gamma_{h\times p}])$, where the γ_i are either zero or one, and we also define a projection matrix Π_Γ which extracts the nonzero components of $\bar{\Gamma}v$, for some vector v

$$\Pi_\Gamma \bar{\Gamma} v = [v_{i_1} \;\; v_{i_2} \;\; \dots \;\; v_{i_{\bar{n}}}]^T \tag{7}$$

and satisfies

$$\Pi_\Gamma^T \Pi_\Gamma = \bar{\Gamma} \quad \Pi_\Gamma \Pi_\Gamma^T = I_{\bar{n}\times\bar{n}} \quad \Pi_\Gamma = \Pi_\Gamma \bar{\Gamma}.$$

Matrices $\bar{\Gamma}_m$, $\bar{\Gamma}_r$, $\bar{\Omega}$ and Π_{Γ_m}, Π_{Γ_r}, Π_Ω are defined in the same manner. Similarly to $y(t)$, the values of $r(t)$ at sampling instants t_k will be denoted by $\tilde{r}_k$ and to take into account the multi-rate nature of the outputs we define $r_k = \Gamma_{rk}\tilde{r}_k$. We can then introduce the error variables $\tilde{e}_k = \tilde{y}_{rk} - \tilde{r}_k$ and $e_k = y_{rk} - r_k$.

2.3. Problem Statement

Given this setup the problem addressed in this paper can be stated as follows:
Problem statement:

I. For a fixed operating point α_0, find a possibly time-varying discrete-time linear controller $C(\alpha_0) : [y_{m\delta k}, e_{\delta k}] \to u_{\delta k}$

$$C(\alpha_0) = \left\{ \begin{bmatrix} x^c_{\delta k+1} \\ u_{\delta k} \end{bmatrix} = \begin{bmatrix} A^c_k(\alpha_0) & B^c_{1k}(\alpha_0) & B^c_{2k}(\alpha_0) \\ C^c_k(\alpha_0) & D^c_{1k}(\alpha_0) & D^c_{2k}(\alpha_0) \end{bmatrix} \begin{bmatrix} x^c_{\delta k} \\ y_{\delta mk} \\ e_{\delta k} \end{bmatrix} \right. \tag{8}$$

for the linearization of the nonlinear plant (4) with interface (5) that stabilizes the resulting closed-loop system and achieves zero steady-state error for e_k, where $u_{\delta k} = u_k - u_0$, $y_{m\delta k} = y_{mk} - \Gamma_{mk} y_{m0}$, $y_{m0} = h_m(x_0, w_0)$ and $e_{\delta k} = e_k$.

II. Based on the family of linear controllers $C(\alpha_0)$, implement a discrete-time controller K, possibly nonlinear and time-varying, that satisfies the linearization property and takes the form

$$K = \left\{ \begin{array}{rcl} x^c_{k+1} = & f_c(x^c_k, y_{mk}, e_k, \alpha_k, k) \\ u_k = & h_c(x^c_k, y_{mk}, e_k, \alpha_k, k) \end{array} \right., \tag{9}$$

where $x^c_k \in \mathbb{R}^{n_K}$, and for a given k, f_c and h_c are continuously differentiable functions of their arguments. Given its dependence on α_k, the scheduling variable sampled at time t_k, K is referred to as a gain-scheduled controller. By linearization property we formally mean that if we consider a family Σ_c of equilibrium points for the controller compatible with Σ, defined in (2), such that

$$\begin{aligned} \Sigma_c = \{x^c_0 : x^c_0 = f_c(x^c_0, y_{m0}, 0, \alpha_0, k), \;\; u_0 = h_c(x^c_0, y_{m0}, 0, \alpha_0, k), \;\; y_{m0} = h_m(x_0, w_0) \\ \text{and} \;\; (x_0, u_0, w_0) = a(\alpha_0), \alpha_0 \in \Xi\}, \end{aligned} \tag{10}$$

the controller K linearizes to $C(\alpha_0)$, at each equilibrium point α_0, that is,

$$\begin{array}{rcl} \dfrac{\partial f_c}{\partial x^c}(a_c(\alpha_0), k) & = & A^c_k(\alpha_0) \;\; \dfrac{\partial f_c}{\partial y_m}(a_c(\alpha_0), k) = B^c_{1k}(\alpha_0) \;\; \dfrac{\partial f_c}{\partial e}(a_c(\alpha_0), k) = B^c_{2k}(\alpha_0) \\ \dfrac{\partial h_c}{\partial x^c}(a_c(\alpha_0), k) & = & C^c_k(\alpha_0) \;\; \dfrac{\partial h_c}{\partial y_m}(a_c(\alpha_0), k) = D^c_{1k}(\alpha_0) \;\; \dfrac{\partial h_c}{\partial e}(a_c(\alpha_0), k) = D^c_{2k}(\alpha_0), \\ & & a_c(\alpha_0) = (x^c_0, y_{m0}, 0, \alpha_0) \end{array}$$

In Section 3 we propose a controller structure that solves Part I of the problem statement. This structure renders a simple implementation for the controller, which is described in Section 4, where we prove that the linearization property is verified for this implementation (Part II of the problem statement).

3. REGULATOR STRUCTURE

In this section we focus on proving the existence of a linear controller for the system G_l defined in (4)), with interface SH, given by (5), that achieves closed loop stability and zero steady-state error for the desired outputs. To simplify the notation, both the dependency on α_0, which here is assumed a constant parameter, and the δ subscript, which indicates deviation from equilibrium variables, are dropped. For example, we will use A instead of $A(\alpha_0)$ and $x(t)$ instead of $x_\delta(t)$. We will come back to this local point of view at the end of the section. Furthermore, since $w(t)$, $z(t)$, and the associated matrices play no role in stability and regulation issues, they will also be temporarily disregarded. The equations for the plant are then simply given by

$$G_l = \begin{cases} \dot{x}(t) = Ax(t) + B_2 u(t) \\ y(t) = \begin{bmatrix} y_m(t) \\ y_r(t) \end{bmatrix} = C_2 x(t) = \begin{bmatrix} C_m \\ C_r \end{bmatrix} x(t) \end{cases} \tag{11}$$

Due to the periodic nature of the multi-rate sample and hold devices some of the systems involved in this paper will be linear periodically time-varying, and therefore we first review some of the results regarding periodic systems. Then we present an existing solution for the regulation of multi-rate square linear systems and propose a solution for the regulation of non-square systems.

3.1. Periodic systems theoretical background

Consider the discrete-time linear periodic system

$$P = \begin{cases} x_{k+1} = A_k x_k + B_k u_k \\ y_k = C_k x_k + D_k u_k \end{cases} \tag{12}$$

with initial time $k = 0$ and initial condition x_0 and where A_k, B_k, C_k, and D_k are h-periodic matrices, for example, $A_k = A_{k+h}$. The lifted time-invariant system $\bar{P}$ associated with P is defined as

$$\bar{P} = \begin{cases} \bar{x}_{l+1} = \bar{A}\bar{x}_l + \bar{B}\bar{u}_l \\ \bar{y}_l = \bar{C}\bar{x}_l + \bar{D}\bar{u}_l \end{cases} \tag{13}$$

where $\bar{x}_l = x_{lh}$, $\bar{u}_l = \begin{bmatrix} u_{lh}^T & u_{lh+1}^T & \dots & u_{lh+h-1}^T \end{bmatrix}^T$, $\bar{y}_l = \begin{bmatrix} y_{lh}^T & y_{lh+1}^T & \dots & y_{lh+h-1}^T \end{bmatrix}^T$, and the system matrices are given by $\bar{A} = \Phi(h,0)$, $\bar{B} = [\Phi(h,1)B_0 \ \Phi(h,2)B_1 \dots B_{h-1}]$, $\bar{C} = [C_0^T \ (C_1\Phi(1,0))^T \dots (C_{h-1}\Phi(h-1,0))^T]^T$, and $\bar{D} = d_{ij}$, $d_{ij} = \begin{cases} C_{i-1}\Phi(i-1,j)B_{j-1} & i > j \\ D_i & i = j \\ 0 & i < j \end{cases}$

where $\Phi(i,j)$, is the transition matrix defined such that $\Phi(i,j) = A_{i-1}A_{i-2}\dots A_j$, for $i > j$ and $\Phi(i,i) = I$.

The system P is asymptotically stable, if and only if $\bar{P}$ is asymptotically stable or equivalently if all the eigenvalues of matrix $\bar{A}$ have norm less that one $\|\lambda_i(\bar{A})\| < 1, \ \forall i$. These eigenvalues are called the characteristic multipliers of system P. Detectability and stabilizability are defined in the following way.

Definition 3.1. *The periodic system P is said to be stabilizable if there exists a set of periodic matrices F_k, $F_k = F_{k+h}$, such that $x_{k+1} = (A_k + B_k F_k)x_k$ is stable and it is said to be detectable if there exists a set of periodic matrices G_k, $G_k = G_{k+h}$, such that $x_{k+1} = (A_k + G_k C_k)x_k$ is stable.*

Similarly to stability, these conditions can be verified using the lifted LTI system $\bar{P}$ as stated in the following result.

Lemma 1. *The periodic system P is detectable (stabilizable) if and only if $\bar{P}$ is detectable (stabilizable).*

Proof 1. *See [1].*

The following is also true for periodic systems.

Lemma 2. *The periodic system P is detectable and stabilizable if and only if there exists a periodic linear controller $K_p : y_k \to u_k$ such that the closed loop system is asymptotically stable.*

Proof 2. *See [3].*

3.2. Regulation of multi-rate systems for square plants

For continuous-time and discrete-time single-rate systems, it is well-known that zero-error regulation for constant references of a number of outputs no greater than the number of inputs can be achieved by incorporating in the controller system a number of integrators equal to the number of tracking variables [8]. Regulation for constant references is not tied in with linearity and is achieved even in the presence of model uncertainties that do not affect closed loop stability. These integrators are usually placed after the system, directly integrating the regulated errors [10], [12]. For the discrete-time multi-rate output regulation problem the structure depicted in Figure 2 is proposed in [5] for a square system[†], which can be interpreted as a particular case of (11) with $n_{y_m} = 0$, $n_{y_r} = p$, $m = p$, $C_r = C_2$. The block C_I represents a periodically time-varying system whose state space description is given by

$$C_I = \begin{cases} x^I_{k+1} = x^I_k + \Omega_k u^I_k \\ y^I_k = x^I_k + \Omega_k u^I_k \end{cases} \tag{14}$$

and that integrates its input at the sampling instants at which the hold operation is active. The block C_K represents a linear controller that, in general, is required to be periodically time-varying. Notice that, in this case, integral action is applied at the input of the plant, because directly integrating the error would produce a non-constant signal at the plant's input, given that C_K is generally time-varying.

As expected, integral action plays the key role in achieving zero-output regulation. In [5] it is proved that, under mild assumptions, the augmented system seen by the controller C_K is detectable and stabilizable. By Lemma 2 there exists a controller C_K that asymptotically stabilizes the closed loop system. The system trajectories will therefore converge to the unique

[†]Some small modifications have been made, namely notation and considering a slightly different system for integral action, C_I. These changes however do not impact on the ideas and results presented in [5].

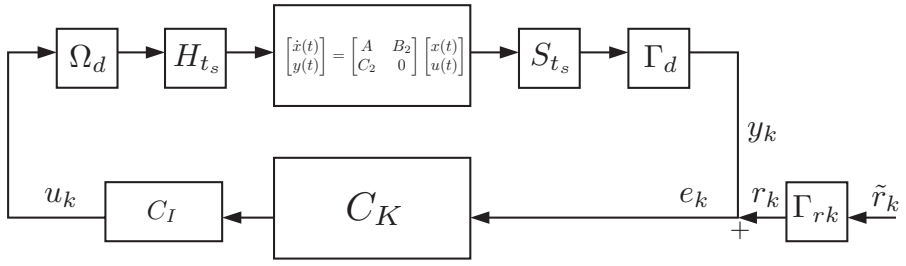

Figure 2. Regulator structure for square systems

equilibrium point that due to integral action and under the assumption that the discretization of G_l given in (11) has no transmission zeros at $z = 1$, is characterized by $u_k = u_0$ and $y_{rk} = \Gamma_k r_0$, $y_r(t) = r_0$.

3.3. Regulation for non-square plants

For a large class of control problems the number of available outputs is greater than the number of actuators. This is generally the case for guidance and control problems for autonomous vehicles. It is well-known that in general we can only impose zero steady-state error for a number of outputs no greater than the number of inputs [8]. However we would like to take advantage of all the available outputs for control and not just the ones for which we require zero steady-state error. Besides improving the transient response, the use of the remaining outputs can be in fact necessary in many applications to guarantee the detectability of the system. In general, assuming uncertainty on the coefficients of the matrices describing the plant, the remaining outputs of the plant y_{mk} have constant but unknown values at steady-state. Motivated by this discussion and by the velocity implementation [11], which will be described shortly, the regulator structure in Figure 3 is proposed.

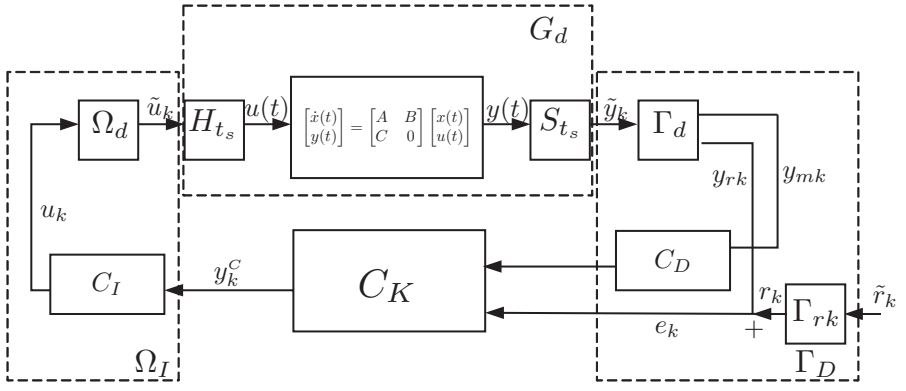

Figure 3. Regulator structure for non-square systems

The periodic system C_D has state space realization given by

$$C_D = \begin{cases} x^D_{k+1} = (I - \Gamma_{mk})x^D_k + \Gamma_{mk} y_{mk} \\ y^D_k = -\Gamma_{mk} x^D_k + \Gamma_{mk} y_{mk} \end{cases} . \tag{15}$$

This system has the role of differentiating the output y_m at sampling instants at which the sampling operation is active. At steady-state the constant unknown values y_{m0} are differentiated bypassing the need to feedforward these values.

The system G_a seen by the controller C_K to be synthesized (see Figure 3) is given by $G_a = \Gamma_D G_d \Omega_I$ where *i)* Ω_I comprises the multi-rate input system Ω_d and periodic integrator C_I, *ii)* G_d the linear system with sample-hold interface and *iii)* Γ_D the multi-rate output system Γ_d and differentiator C_D.

The operations of systems Ω_d and C_I can be combined to yield the simple description of Ω_I, which is the same as C_I, i.e.,

$$\Omega_I = \begin{cases} x^I_{k+1} = x^I_k + \Omega_k y^C_k \\ \tilde{u}_k = x^I_k + \Omega_k y^C_k \end{cases}$$

The equations for $G_d = S_{t_s} G_l H_{t_s}$ can be written as

$$G_d = \begin{cases} x_{k+1} = A_d x_k + B_d \tilde{u}_k \\ \tilde{y}_k = \begin{bmatrix} \tilde{y}_{mk} \\ \tilde{y}_{rk} \end{bmatrix} = C_d x_k = \begin{bmatrix} C_{dm} \\ C_{dr} \end{bmatrix} x_k \end{cases} \tag{16}$$

where $A_d = e^{At_s}$, $B_d = \int_0^{t_s} e^{A\tau} d\tau B_2$ and $C_d = C_2$. Finally the equations for Γ_D are

$$\Gamma_D = \begin{cases} x^D_{k+1} = (I - \Gamma_{mk})x^D_k + \begin{bmatrix} \Gamma_{mk} & 0 \end{bmatrix} \begin{bmatrix} \tilde{y}_{mk} \\ \tilde{e}_k \end{bmatrix} \\ y^D_k = \begin{bmatrix} -\Gamma_{mk} \\ 0 \end{bmatrix} x^D_k + \begin{bmatrix} \Gamma_{mk} & 0 \\ 0 & \Gamma_{rk} \end{bmatrix} \begin{bmatrix} \tilde{y}_{mk} \\ \tilde{e}_k \end{bmatrix} \end{cases}$$

Computing the series of these three systems we obtain

$$G_a = \begin{cases} \begin{bmatrix} x_{k+1} \\ x^I_{k+1} \\ x^D_{k+1} \end{bmatrix} = \begin{bmatrix} A_d & B_d & 0 \\ 0 & I & 0 \\ \begin{bmatrix} \Gamma_{mk} & 0 \end{bmatrix} C_d & 0 & (I - \Gamma_{mk}) \end{bmatrix} \begin{bmatrix} x_k \\ x^I_k \\ x^D_k \end{bmatrix} + \begin{bmatrix} B_d \Omega_k \\ \Omega_k \\ 0 \end{bmatrix} y^C_k \\ y^A_k = \left[\begin{bmatrix} \Gamma_{mk} & 0 \\ 0 & \Gamma_{rk} \end{bmatrix} C_d \quad 0 \quad \begin{bmatrix} -\Gamma_{mk} \\ 0 \end{bmatrix} \right] \begin{bmatrix} x_k \\ x^I_k \\ x^D_k \end{bmatrix} + \begin{bmatrix} 0 \\ -\Gamma_{rk} \end{bmatrix} \tilde{r}_k \end{cases} \tag{17}$$

The next theorem states sufficient conditions under which the system G_a is detectable and stabilizable that only depend on the original discrete-time plant G_d, described by (16).

Theorem 1. *Assume that the following conditions hold*

i) (A_d, B_d) *is stabilizable and* (A_d, C_d) *is detectable.*
ii) Each output is sampled and each input is updated at least once in a period T, i.e., $\forall_i \exists_{k \in \{1,\ldots,h\}} : (\Gamma_k)_{ii} = 1$ *and* $\forall_i \exists_{k \in \{1,\ldots,h\}} : (\Omega_k)_{ii} = 1$.
iii) If there exists $\lambda_k(A_d) = \lambda_k$ *such that* $\|\lambda_k\| = 1$ *then* $\lambda_k^h \neq 1$*, and if there exists a pair* $\lambda_i(A_d) = \lambda_i$*,* $\lambda_j(A_d) = \lambda_j$ *such that* $\lambda_i \neq \lambda_j$*,* $\|\lambda_i\| \geq 1$ *and* $\|\lambda_j\| \geq 1$ *then* $\lambda_j^h \neq \lambda_i^h$.

iv) There are no transmission zeros at $z = 1$ from the input of G_d to the regulated output, i.e.,

$$\begin{bmatrix} A_d - I & B_d \\ C_{dr} & 0 \end{bmatrix} \tag{18}$$

is full rank.

Then, the augmented periodic system G_a is detectable and stabilizable.

Proof 3. *See Appendix.*

By Lemma 2 detectability and stabilizability guarantees the existence of an asymptotic stabilizing controller for the augmented system G_a. Due to the previous discussion, the following theorem comes as no surprise.

Lemma 3. *Consider the feedback interconnection of G_a and C_K and suppose the controller C_K asymptotically stabilizes the resulting closed loop system. Then, zero-error output regulation for $y_r(t)$ is achieved even in the presence of plant perturbations, provided that closed-loop stability is preserved.*

Proof 4. *See Appendix.*

3.4. Solution to Part I of the Problem Statement

Suppose that the state space realization of an asymptotically stabilizing controller C_K for plant G_a is given by

$$C_K = \left\{ \begin{bmatrix} x_{k+1}^K \\ y_k^K \end{bmatrix} = \begin{bmatrix} A_k^K & B_{1k}^K & B_{2k}^K \\ C_k^K & D_{1k}^K & D_{2k}^K \end{bmatrix} \begin{bmatrix} x_k^K \\ y_k^D \\ e_k \end{bmatrix} \right. \tag{19}$$

Returning to the original problem, stated in Part I of the problem statement, of finding a local controller, with the properties referred therein, we rewrite the equations for C_I, C_K, and C_D in the form

$$C(\alpha_0) = \left\{ \begin{array}{l} \begin{bmatrix} x_{\delta k+1}^K \\ y_{\delta k}^K \end{bmatrix} = \begin{bmatrix} A_k^K(\alpha_0) & B_{1k}^K(\alpha_0) & B_{2k}^K(\alpha_0) \\ C_k^K(\alpha_0) & D_{1k}^K(\alpha_0) & D_{2k}^K(\alpha_0) \end{bmatrix} \begin{bmatrix} x_{\delta k}^K \\ y_{\delta k}^D \\ e_{\delta k} \end{bmatrix} \\ \begin{bmatrix} x_{\delta k+1}^D \\ y_{\delta k}^D \end{bmatrix} = \begin{bmatrix} I - \Gamma_{mk} & \Gamma_{mk} \\ -\Gamma_{mk} & \Gamma_{mk} \end{bmatrix} \begin{bmatrix} x_{\delta k}^D \\ y_{m\delta k} \end{bmatrix} \\ \begin{bmatrix} x_{\delta k+1}^I \\ u_{\delta k} \end{bmatrix} = \begin{bmatrix} I & \Omega_k \\ I & \Omega_k \end{bmatrix} \begin{bmatrix} x_{\delta k}^I \\ y_{\delta k}^K \end{bmatrix} \end{array} \right. \tag{20}$$

where we have added the dependency on α_0 and the notation indicating that it is a local controller, for example, $x_{\delta k}^K$ instead of x_k^K. These equations can be combined to yield

$$C(\alpha_0) = \left\{ \begin{bmatrix} x_{\delta k+1}^c \\ u_{\delta k} \end{bmatrix} = \begin{bmatrix} A_k^c(\alpha_0) & B_{1k}^c(\alpha_0) & B_{2k}^c(\alpha_0) \\ C_k^c(\alpha_0) & D_{1k}^c(\alpha_0) & D_{2k}^c(\alpha_0) \end{bmatrix} \begin{bmatrix} x_{\delta k}^c \\ y_{m\delta k} \\ e_{\delta k} \end{bmatrix} \right. \tag{21}$$

where $x_{\delta k}^c = [(x_{\delta k}^K)^T \ (x_{\delta k}^D)^T \ (x_{\delta k}^I)^T]^T$ and

$$A_k^c(\alpha_0) = \begin{bmatrix} A_k^K(\alpha_0) & -B_{1k}^K(\alpha_0)\Gamma_{mk} & 0 \\ 0 & I-\Gamma_{mk} & 0 \\ \Omega_k C_k^K(\alpha_0) & -\Omega_k D_{1k}^K(\alpha_0)\Gamma_{mk} & I \end{bmatrix} \quad B_{1k}^c(\alpha_0) = \begin{bmatrix} B_{1k}^K(\alpha_0)\Gamma_{mk} \\ \Gamma_{mk} \\ \Omega_k D_{1k}^K(\alpha_0)\Gamma_{mk} \end{bmatrix}$$

$$B_{2k}^c(\alpha_0) = \begin{bmatrix} B_{2k}^K(\alpha_0) \\ 0 \\ \Omega_k D_{2k}^K(\alpha_0) \end{bmatrix} \quad C_k^c(\alpha_0) = \begin{bmatrix} \Omega_k C_k^K(\alpha_0) & -\Omega_k D_{1k}^K(\alpha_0)\Gamma_{mk} & I \end{bmatrix}$$

$$D_{1k}^c(\alpha_0) = \begin{bmatrix} \Omega_k D_{1k}^K(\alpha_0)\Gamma_{mk} \end{bmatrix} \quad D_{2k}^c(\alpha_0) = \begin{bmatrix} \Omega_k D_{2k}^K(\alpha_0) \end{bmatrix} \tag{22}$$

which is a solution to Part I of the problem statement.

4. GAIN-SCHEDULING IMPLEMENTATION

The controller structure obtained in the last section is especially suited for a gain-scheduling implementation that satisfies the linearization property, described in Part II of the problem statement. We present next this implementation and establish its connection with the velocity implementation, which is a methodology for the discrete-time single-rate case to implement a gain-scheduling controller that satisfies the referred linearization property.

4.1. Gain-scheduling implementation

Having designed the parameterized family of linear controllers $C(\alpha_0)$, (20), suppose we implement the gain-scheduled non-linear controller K as follows

$$K(\alpha_k) = \begin{cases} \begin{bmatrix} x_{k+1}^K \\ y_k^K \end{bmatrix} = \begin{bmatrix} A_k^K(\alpha_k) & B_{1k}^K(\alpha_k) & B_{2k}^K(\alpha_k) \\ C_k^K(\alpha_k) & D_{1k}^K(\alpha_k) & D_{2k}^K(\alpha_k) \end{bmatrix} \begin{bmatrix} x_k^K \\ y_k^D \\ e_k \end{bmatrix} & (23.1) \\ \begin{bmatrix} x_{k+1}^D \\ y_k^D \end{bmatrix} = \begin{bmatrix} I-\Gamma_{mk} & \Gamma_{mk} \\ -\Gamma_{mk} & \Gamma_{mk} \end{bmatrix} \begin{bmatrix} x_k^D \\ y_{mk} \end{bmatrix} & (23.2) \\ \begin{bmatrix} x_{k+1}^I \\ u_k \end{bmatrix} = \begin{bmatrix} I & \Omega_k \\ I & \Omega_k \end{bmatrix} \begin{bmatrix} x_k^I \\ y_k^K \end{bmatrix} & (23.3) \\ \alpha_k = v(\tilde{y}_k, w_k) & (23.4) \\ \begin{bmatrix} x_{k+1}^Y \\ \tilde{y}_k \end{bmatrix} = \begin{bmatrix} I-\Gamma_k & \Gamma_k \\ I-\Gamma_k & \Gamma_k \end{bmatrix} \begin{bmatrix} x_k^Y \\ y_k \end{bmatrix} & (23.5) \end{cases} \tag{23}$$

Notice that α_k, which was considered to be a constant parameter during the design process, now becomes a scheduling variable computed on-line from the plant outputs and exogenous variables. Due to the multi-rate nature of the output, the system described by (23.5) is used to perform a hold operation on the output y_k so that the scheduling variable α_k is computed, at each iteration, according to the last sampled value of the output. The exogenous vector is assumed available at each sampling instant, so that $w_k = w(t_k)$. Notice that the non-linear controller proposed in (23) conforms to the general description of K given in (9), with $x_k^c = [(x_k^K)^T \ (x_k^D)^T \ (x_k^I)^T]$,

$$f_c(x_k^c, y_{mk}, e_k, \alpha_k, k) = \begin{bmatrix} A_k^K(\alpha_k) & -B_{1k}^K(\alpha_k)\Gamma_{mk} & 0 \\ 0 & I - \Gamma_{mk} & 0 \\ \Omega_k C_k^K(\alpha_k) & -\Omega_k D_{1k}^K(\alpha_k)\Gamma_{mk} & I \end{bmatrix} \begin{bmatrix} x_k^K \\ x_k^D \\ x_k^I \end{bmatrix} + \begin{bmatrix} B_{1k}^K(\alpha_k)\Gamma_{mk} & B_{2k}^K(\alpha_k) \\ \Gamma_{mk} & 0 \\ \Omega_k D_{1k}^K(\alpha_k)\Gamma_{mk} & \Omega_k D_{2k}^K(\alpha_k) \end{bmatrix} \begin{bmatrix} y_{mk} \\ e_k \end{bmatrix}, \quad (24)$$

and

$$h_c(x_k^c, y_{mk}, e_k, \alpha_k, k) = \begin{bmatrix} \Omega_k C_k^K(\alpha_k) & -\Omega_k D_{1k}^K(\alpha_k)\Gamma_{mk} & I \end{bmatrix} \begin{bmatrix} x_k^K \\ x_k^D \\ x_k^I \end{bmatrix} + \begin{bmatrix} \Omega_k D_{1k}^K(\alpha_k)\Gamma_{mk} & \Omega_k D_{2k}^K(\alpha_k) \end{bmatrix} \begin{bmatrix} y_{mk} \\ e_k \end{bmatrix}. \quad (25)$$

The next theorem establishes that, at each equilibrium characterized by α_0, the nonlinear controller K linearizes to the designed controller $C(\alpha_0)$, and therefore K constitutes a solution to Part II of the problem statement.

Theorem 2. *Suppose for each parameter vector $\alpha_0 \in \Xi$, the feedback interconnection of the linearized system $G_l(\alpha_0)$, described by (4), and the designed controller $C(\alpha_0)$, described by (8), with multi-rate sample-data interface is asymptotically stable. Then the feedback interconnection of the multi-rate nonlinear system and gain-scheduled controller K, described by (23), admits a unique equilibrium point associated with α_0 and the linearization of K, about this equilibrium coincides with the designed controller $C(\alpha_0)$, given by (20).*

Proof 5. *It is easy to verify that the equilibrium points for (23) defined in (10) are*

$$\underline{x}^K = 0,\ \underline{y}^K = 0,\ \underline{x}^D = y_{m0},\ \underline{y}^D = 0,\ \underline{x}^I = u_0,\ \underline{e} = 0,\ \underline{u} = u_0. \quad (26)$$

Due to asymptotic stability and the linearity of the controller for each fixed value of the parameter, these are the unique equilibrium points of the controller compatible with those of the plant Σ. Defining the matrix

$$M(\alpha_k) = \begin{bmatrix} A_k^K(\alpha_k) & B_{1k}^K(\alpha_k) & B_{2k}^K(\alpha_k) \\ C_k^K(\alpha_k) & D_{1k}^K(\alpha_k) & D_{2k}^K(\alpha_k) \end{bmatrix}$$

the linearization of (23) *about* (26) *can be written as*

$$K_l = \left\{ \begin{array}{l} \begin{bmatrix} x^K_{\delta k+1} \\ y^K_{\delta k} \end{bmatrix} = M(\alpha_k) \begin{bmatrix} x^K_{\delta k} \\ y^D_{\delta k} \\ e_{\delta k} \end{bmatrix} + \\ \underbrace{\frac{\partial}{\partial \alpha_k}(M(\alpha_k) \begin{bmatrix} x^K_k \\ y^D_k \\ e_k \end{bmatrix})(\frac{\partial v(\tilde{y}_k, w_k)}{\partial \tilde{y}_k}\tilde{y}_{\delta k} + \frac{\partial v(\tilde{y}_k, w_k)}{\partial w_k} w_{\delta k})}_{H.C.T} \\ \begin{bmatrix} x^D_{\delta k+1} \\ y^D_{\delta k} \end{bmatrix} = \begin{bmatrix} I - \Gamma_{mk} & \Gamma_{mk} \\ -\Gamma_{mk} & \Gamma_{mk} \end{bmatrix} \begin{bmatrix} x^D_{\delta k} \\ y_{\delta mk} \end{bmatrix} \\ \begin{bmatrix} x^I_{\delta k+1} \\ u_{\delta k} \end{bmatrix} = \begin{bmatrix} I & \Omega_k \\ I & \Omega_k \end{bmatrix} \begin{bmatrix} x^I_{\delta k} \\ y^K_{\delta k} \end{bmatrix} \\ \begin{bmatrix} x^Y_{\delta k+1} \\ \tilde{y}_{\delta k} \end{bmatrix} = \begin{bmatrix} I - \Gamma_k & \Gamma_k \\ I - \Gamma_k & \Gamma_k \end{bmatrix} \begin{bmatrix} x^Y_{\delta k} \\ y_{\delta k} \end{bmatrix} \end{array} \right.$$

where H.C.T are the hidden coupling terms which result from introducing the scheduling variable α_k*. Due to the special structure of the controller these terms cancel out when evaluated at the equilibrium* (26) *since all its components are multiplied by one of the components of* x^K_k*,* y^D_k*, of* e_k*, which are zero at equilibrium. The linearizations reduces then to* (20) *concluding the proof.*

4.2. Connection with the velocity implementation

The velocity implementation, presented in [11], is a method for implementing a gain-scheduled controller with integral action that satisfies the linearization property. For the discrete-time single-rate case, see [10]. The method can be briefly explained as follows. Suppose that for a family of linear discrete-time single-rate plants one has designed a family of linear controllers with the structure

$$C(\alpha_0) = \left\{ \begin{array}{l} \left. \begin{array}{l} x^K_{\delta k+1} = A^K(\alpha_0)x^K_{\delta k} + B^K_1(\alpha_0)y_{m\delta k} + B^K_2(\alpha_0)y^I_{\delta k} \\ u_{\delta k} = C^K(\alpha_0)x^K_{\delta k} + D^K_1(\alpha_0)y_{m\delta k} + D^K_2(\alpha_0)y^I_{\delta k} \end{array} \right\} C_d(\alpha_0) \\ x^I_{\delta k+1} = x^I_{\delta k} + (y_{r\delta k} - r_{\delta k}) \\ y^I_{\delta k} = x^I_{\delta k} + (y_{r\delta k} - r_{\delta k}) \end{array} \right.$$

where we consider a non-strictly proper integrator to conform with the present formulation. Suppose also that we implement the non-linear controller moving the integrators to the front of the controller (input of the plant) as shown in Figure 4. Again, α_k which was assumed constant throughout the design process, becomes a time-varying scheduling variable through the dependence $\alpha_k = v(y_k, w_k)$. The equations for this implemented controller are

$$K(\alpha_k) = \left\{ \begin{array}{l} x^K_{k+1} = A^K(\alpha_k)x^K_k + B^K_1(\alpha_k)(y_{mk} - y^D_k) + B^K_2(\alpha_k)(y_{rk} - r_k) \\ x^I_{k+1} = x^I_k + C^K(\alpha_k)x^K_k + D^K_1(\alpha_k)(y_{mk} - y^D_k) + D^K_2(\alpha_k)(y_{rk} - r_k) \\ x^D_{k+1} = y_{mk} \\ y^D_k = x^D_k \\ \alpha_k = v(y_k, w_k) \\ u_k = x^I_k + C^K(\alpha_k)x^K_k + D^K_1(\alpha_k)(y_{mk} - y^D_k) + D^K_2(\alpha_k)(y_{rk} - r_k) \end{array} \right.$$

The idea behind moving the integrators is that of building a linear equivalent controller for constant parameter values that when implemented as a nonlinear controller gain-scheduled

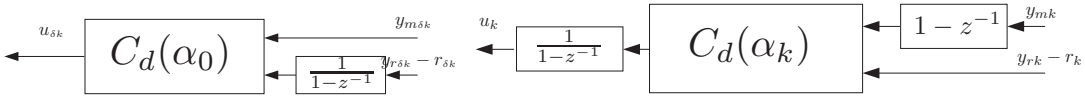

(a) Designed Controller (b) Implemented Controller

Figure 4. Velocity implementation

on α_k satisfies the linearization property. Since at equilibrium the input of $C_d(\alpha_k)$ is zero-valued, it follows that the so-called hidden coupling terms of the linearized controller, which are due to the introduction of α_k, are all canceled out (this argument was also the basis for proving Theorem 2). It is easy to see that in general this does not occur for other controller implementations (see [11], [12], [16] for examples).

There is a close relationship between the velocity implementation and the method presented herein when the multi-rate setup is particularized to the single-rate case. In the single rate case we have $\Gamma_k = I, \ \forall_k$ and $\Omega_k = I \ \forall_k$, from which equations (14) and (15) reduce to simple integrators and differentiators and therefore the controller described by (20) acquires the same structure as that shown in Figure 4(b). However the point of view is somewhat different. While in the velocity implementation method, the controller could be synthesized by augmenting the state with the integrators at the front of the plant, which includes, for example, P.I. controllers when the state is available, the same principle can not be applied in the multi-rate case. Instead, the synthesized controller takes into account in the design the differentiator at the output and the integrators at the input of the plant. Nevertheless we stress that we do not make any assumption on how the controller is synthesized either for the multi-rate case or for the particular case of single-rate (Lemma 2 assures that a stabilizing controller exists) and that the set of stabilizing controllers for either one of the single-rate structures show in Figure 4 is the same, when frozen-time values of the parameters are considered.

4.3. Outline of the proposed method

The following procedure outlines the method proposed for the design and implementation of gain-scheduled controllers for multi-rate systems:

1. Given a nonlinear system in the form described by (1), with multi-rate input and output interface SH described by (5), obtain a family of parameter-dependent linear models in the form (4).
2. Design a family of linear controllers with the structure (21) and (22). Theorem 1 along with Lemma 2 guarantee that for each fixed value of the schedule parameter a stabilizing controller exists, under mild assumptions.
3. Implement the non-linear gain-scheduled controller according to (23). Theorem 2 assures that the linearization property is verified.

5. Trajectory tracking control for autonomous rotorcraft

In this section the proposed method is applied to the control of an autonomous rotorcraft. To this effect, the dynamics model of a small-scale helicopter, parameterized for the Vario X-treme R/C helicopter [7], is used. We address a trajectory tracking control problem, which can be described as the problem of steering a vehicle along a predefined trajectory defined in terms of space and time coordinates. The solution presented relies on the definition of an adequate error space to express the model of the vehicle [17]. The following section briefly describes the helicopter dynamic model.

5.1. Vehicle Dynamic Model

The helicopter dynamics are described using the conventional six degree of freedom rigid body equations

$$\begin{cases} \dot{v} = f\left(v,\, \omega,\, u\right) + \mathcal{R}^{-1}(\lambda)[0\ 0\ g]^{T} \\ \dot{\omega} = n\left(v,\, \omega,\, u\right) \\ \dot{p} = \mathcal{R}(\lambda)v \\ \dot{\lambda} = \mathcal{Q}(\phi_{B}, \theta_{B})\,\omega \end{cases}, \tag{27}$$

where $(p,\ \mathcal{R}) \in SE(3) \triangleq \mathbb{R}^3 \times SO(3)$ denotes the configuration of the body frame $\{B\}$ attached to the vehicle's center of mass with respect to the inertial frame $\{I\}$ and the rotation matrix $\mathcal{R} = \mathcal{R}(\lambda)$ can be parameterized by the Z-Y-X Euler angles $\lambda = [\phi_{B}\ \theta_{B}\ \psi_{B}]^{T}$, $\theta_{B} \in\,]-\pi/2, \pi/2[$, $\phi_{B}, \psi_{B} \in \mathbb{R}$, $\mathcal{R} = R_{Z}(\psi_{B})R_{Y}(\theta_{B})R_{X}(\phi_{B})$. The inertial frame $\{I\}$ is such that its $z-$axis is aligned with the gravity vector. The linear and angular body velocities are denoted by $v = [u_{B}\ v_{B}\ w_{B}]^{T} \in \mathbb{R}^3$ and $\omega = [p_{B}\ q_{B}\ r_{B}]^{T} \in \mathbb{R}^3$, respectively. Notice that the gravitational term $f_{g}(\phi_{B}, \theta_{B}) = \mathcal{R}^{-1}(\lambda)[0\ 0\ g]^{T}$ depends only on the roll and pitch angles and that the euler angles rates $\dot{\lambda}$ and the angular velocities are related by the well-known transformation matrix $\mathcal{Q}(\phi_{B}, \theta_{B})$.

The actuation $u = [\theta_{0}\ \theta_{1s}\ \theta_{1s}\ \theta_{0t}]$ comprises the main rotor collective input θ_{0}, the main rotor cyclic inputs, θ_{1s} and θ_{1c}, and the tail rotor collective input θ_{0t}. The dynamic equations for the helicopter are highly non-linear and its derivation is only accomplishable assuming several simplifications. For a detailed explanation of the modeling of the small-scale helicopter used in this paper the reader is referred to [7].

5.2. Generalized error dynamics

The integrated guidance and control strategy proposed in [17] for the trajectory tracking problem, consists in defining a convenient non-linear transformation to be applied to the vehicle dynamic and kinematic model. In the new error space the trajectory tracking problem is reduced to that of regulating the error variables to zero using the fact that the linearization of the error dynamics is time-invariant about any trimming trajectories. It is well-known that these comprise helix and straight lines, parameterized by the vehicle linear speed, flight path angle, yaw rate and yaw angle with respect to the path [17]. Thus, the control design for the trajectory tracking problem can be solved by using tools that borrow from gain scheduling control theory, where the aforementioned parameters play the role of scheduling variables that

interpolate the parameters of linear controllers designed for a finite number of representative trimming trajectories.

In order to define the non-linear transformation we start by formally introducing the trimming trajectories. Consider the helicopter equations of motion presented in (27), and let v_C, ω_C, p_C, $\lambda_C = [\phi_C \;\; \theta_C \;\; \psi_C]^T$ and u_C denote the trimming values of the state and input vectors, respectively. At trimming, these vectors satisfy $\dot{v}_C = 0$ and $\dot{\omega}_C = 0$, implying that $\dot{u}_C = 0$, $\dot{\phi}_C = 0$ and $\dot{\theta}_C = 0$. Given the dependence of the gravitational terms on the roll and pitch angles, only the yaw angle can change without violating the equilibrium condition. However, ψ_C satisfies

$$\begin{bmatrix} 0 \\ 0 \\ \dot{\psi}_C \end{bmatrix} = \mathcal{Q}(\phi_C, \theta_C)\omega_C$$

and thus the yaw rate $\dot{\psi}_C$ is constant. From this analysis it is easy to show [17] that trimming trajectories correspond to helices (which degenerate into straight lines when $\dot{\psi}_C = 0$) that can be described by

$$\lambda_C = \begin{bmatrix} \phi_C \\ \theta_C \\ \dot{\psi}_C t + \psi_0 + \psi_{CT} \end{bmatrix}, \;\; p_C = \begin{bmatrix} \frac{V_C}{\dot{\psi}_C} \cos(\gamma_C) \sin(\dot{\psi}_C t + \psi_0) \\ -\frac{V_C}{\dot{\psi}_C} \cos(\gamma_C) \cos(\dot{\psi}_C t + \psi_0) \\ -V_C \sin(\gamma_C) t \end{bmatrix} + \begin{bmatrix} x_0 \\ y_0 \\ z_0 \end{bmatrix},$$

where $V_C = \|v_C\|$ is the linear body speed and γ_C is the flight path angle. Therefore, apart from a z-rotation and a translation, the parameter vector $(V_C, \gamma_C, \dot{\psi}_C, \phi_C, \theta_C, \psi_{CT},)$ completely characterizes a trimming trajectory. As explained in [6], due to the tail rotor actuation, helicopters can describe trimming trajectories with arbitrary but constant yaw angle relative to the path, that is, with arbitrary ψ_{CT}. However the roll and pitch angles ϕ_C and θ_C are automatically constrained by this choice. The trimming trajectory can thus be described by the following parameterization

$$\xi_0 = \begin{bmatrix} V_C & \gamma_C & \dot{\psi}_C & \psi_{CT} \end{bmatrix}^T$$

Moreover, introducing $\xi = (V, \gamma, \dot{\psi}, \psi)$

$$V = \|v\| \quad \gamma = \arctan(-\frac{w'_B}{u'_B}) \quad \dot{\psi} = \dot{\psi}_B \quad \psi = \psi_B - \psi_0 \;\; , \qquad \begin{bmatrix} u'_B \\ v'_B \\ w'_B \end{bmatrix} = \mathcal{R} \begin{bmatrix} u_B \\ v_B \\ w_B \end{bmatrix} \tag{28}$$

we have at equilibrium $\xi = \xi_0$. For the sake of simplicity, in this particular case study, the vector ξ_0 is partitioned according to $\xi_0 = (\varphi_0, \alpha_0)$, where $\varphi_0 := (V_C, \dot{\psi}_C, \psi_{CT})$ is constant and $\alpha_0 := \gamma_C$ is allowed to vary. That is, we consider paths formed by the concatenation of trimming trajectories that can be parameterized by α_0 only. By imposing this restriction on the reference trajectories and considering a similar partition for the scheduling variable $\xi = (\varphi, \alpha)$, where $\varphi = (V, \dot{\psi}, \psi)$ and $\alpha = \gamma$, we assume that φ does not change significantly between trajectories. Notice that α conforms with the general description of scheduling variable given in Section 2.

The generalized error vector relating the vehicle state and the commanded trajectory parameterized by ξ_0, or equivalently α_0 since φ_0 is constant, can be defined using the nonlinear

transformation

$$x_e = \begin{bmatrix} v_e \\ \omega_e \\ p_e \\ \lambda_e \end{bmatrix} = \begin{bmatrix} v - v_C \\ \omega - \omega_C \\ \mathcal{R}^{-1}(p_B - p_C) \\ \mathcal{Q}^{-1}(\lambda_B - \lambda_C) \end{bmatrix} \tag{29}$$

Since $\dot{v}_C = 0$ and $\dot{\omega}_C = 0$ for any trimming trajectory, the nonlinear error dynamics can be written as [17]

$$G = \begin{cases} \dot{v}_e = \dot{v} \\ \dot{\omega}_e = \dot{\omega} \\ \dot{p}_e = v_B - \mathcal{R}_e^{-1} v_C - \mathcal{S}(\omega) p_e \\ \dot{\lambda}_e = \omega - \mathcal{Q}^{-1}\mathcal{Q}_C\omega_C - (\frac{d}{dt}\mathcal{Q}^{-1})\mathcal{Q}\lambda_e \end{cases} \tag{30}$$

where $\mathcal{R}_e^{-1} = \mathcal{R}^{-1}\mathcal{R}(\phi_C, \theta_C)$, $\mathcal{Q}_C = \mathcal{Q}(\phi_C, \theta_C)$ and $S(\omega)$ is a skew-symmetric matrix defined such that $\mathcal{S}(\omega) = [\omega\times]$.

The output vector for which we require steady-state tracking is defined as

$$y_{er} = \begin{bmatrix} p_e \\ \psi_e \end{bmatrix} \quad , \quad \psi_e = \begin{bmatrix} 0 & 0 & 1 \end{bmatrix} \lambda_e$$

It is straightforward to obtain that $y_{er} = 0$ implies $x_e = 0$ and that the vehicle will follow the path with the desired linear speed and orientation if and only if $x_e = 0$. As mentioned in the next section, the state is assumed available, although at different rates, and thus we have

$$y_{em} = x_e$$

The linearization of (30) about the equilibrium ($x_e = 0, u = u_C$), or equivalently, the linearization of (27) about α_0, can be written in compact form as

$$G_l(\alpha_0) = \begin{cases} \dot{x}_{e\delta} = A_e(\alpha_0)x_{e\delta} + B_e(\alpha_0)u_\delta \\ y_{em\delta} = x_{e\delta} \\ y_{er\delta} = C_{er}(\alpha_0)x_{e\delta} \end{cases} , \tag{31}$$

where $x_{e\delta} = x_e$, $u_\delta = u - u_C$, $y_{er\delta} = y_{er}$, $y_{em\delta} = y_{em}$, and $C_{er}(\alpha_0) = \begin{bmatrix} 0 & I_3 & 0 \\ 0 & 0 & [0\,0\,1] \end{bmatrix}$. For details on the matrices of the linearization see [17]. With respect to Section 2, $G_l(\alpha_0)$ is the parameterized local system model, described by (4), for which the controller is to be designed.

5.3. Multi-rate characteristics of the sensors

As already mentioned, for an autonomous vehicle the dynamic and kinematic state-variables comprise linear and angular velocities, position and orientation which are usually available at different rates (for example the position is typically measured by a GPS receiver which imposes a slow rate). In the present paper we assume that the state variables of the vehicle corresponding to linear and angular velocities and orientation are measured at a sampling rate of 50 Hz, which corresponds to a sampling period $t_s = 0.02$ s, whereas the position variables are measured at a sampling rate of 2.5 Hz, corresponding to a sampling rate of $t_{sp} = 0.4$ s. The actuators are assumed synchronous and updated at a rate of 50 Hz. According to these

sampling rates, the h-periodic matrices Γ_{mk}, Γ_{rk} and Ω_k that characterize the multi-rate setup, defined in Section 2, are given by

$$\begin{aligned}
\Omega_k &= I_4 \\
\Gamma_{mk} &= \begin{cases} I_{12} & k = 0 \\ \mathrm{diag}([1_3 \;\; 1_3 \;\; 0_3 \;\; 1_3]) & \text{otherwise} \end{cases} \\
\Gamma_{rk} &= \begin{cases} I_4 & k = 0 \\ \mathrm{diag}([0_3 \;\; 1]) & \text{otherwise} \end{cases}, \qquad k = 0, .., h-1.
\end{aligned}$$

where $h = 20$.

5.4. Controller Synthesis and Implementation

The commonly used method for the design of a family of controllers for the parameterized family of models described by (31), which is also adopted in the present paper, comprises the following steps: *i)* obtain a finite set of parameter values from the discretization of the continuous parameter space, *ii)* synthesize a linear controller for each linear plant, described by (31), obtained from the linearization of the nonlinear plant for each value of the schedule parameter, *iii)* interpolate the coefficients of the linear controllers to obtain a continuously parameter-varying controller.

We have restricted the parameter space to $\alpha = \gamma$, which means that the synthesized controllers are valid in operating conditions where the remaining parameters $\varphi = (V, \dot{\psi}, \psi)$ do not change significantly about nominal values $(V_C, \dot{\psi}_C, \psi_C)$. The finite set of values for the discretization of this one-dimensional parameter space was chosen to be

$$\bar{\alpha}_0 = \{\bar{\alpha}_{0i}\} = [\text{-}50 \;\; \text{-}40 \;\; \text{-}30 \;\; \text{-}20 \;\; \text{-}10 \;\; 0 \;\; 10 \;\; 20 \;\; 30 \;\; 40 \;\; 50] \frac{\pi}{180} \;\; \text{rad.}$$

so that the conditions under which the vehicle is expected to operate include straight lines $\dot{\psi}_C = 0$ and z-aligned helices $\dot{\psi}_C \neq 0$, with a flight path angle between -50 and 50 degrees, that the vehicle is required to follow with constant velocity, yaw rate and orientation with respect to the path $((V, \dot{\psi}, \psi) = (V_C, \dot{\psi}_C, \psi_C))$.

For each fixed value of α_0, the standard output feedback $\mathcal{H}_2$ formulation for periodic system was used to synthesize a controller C_K for the augmented system G_a, described by (17), where A_d, B_d, C_d are the discretizations of system matrices of (31). Notice that G_a has a number of states equal to $n + m + n_{y_r} = 12 + 4 + 12 = 28$ and a number of outputs equal to $n_{y_m} + n_{y_r} = 12 + 4 = 16$. For an h-periodic system G of the form

$$G := \begin{cases} x_{k+1} = A_k x_k + B_{1k} w_k + B_{2k} u_k \\ z_k = C_{1k} x_k + D_{11k} w_k + D_{12k} u_k \\ y_k = C_{2k} x_k + D_{21k} w_k + D_{22k} u_k \end{cases} \tag{32}$$

with $D_{11k} = 0$, the $\mathcal{H}_2$ control problem can be interpreted as the problem of finding a linear h-periodic controller $K : y_k \mapsto u_k$ that minimizes the average over one period of the norms of the impulse responses of the closed-loop system,

$$G_{cl} := \begin{cases} \underline{\mathrm{x}}_{k+1} = \underline{\mathrm{A}}_k \underline{\mathrm{x}}_k + \underline{\mathrm{B}}_{1k} w_k \\ z_k = \underline{\mathrm{C}}_{1k} \underline{\mathrm{x}}_k \end{cases}$$

which can be written as

$$\|G_{cl}\|_2 = (\frac{1}{h}\sum_{j=0}^{h-1}\sum_{i=1}^{n_w}\|G_{cl}\delta(k-j)e_i\|_2)^{\frac{1}{2}}. \tag{33}$$

where $G_{cl}\delta(k-j)e_i$ denotes the output response to an impulse applied at input i and time j. The solution to this problem can be obtained by solving two periodic Riccati equations [2] or by the solution of two LMI optimization problems [19]. The matrices associated with the performance channel $w_k \mapsto z_k$ are typically used as tuning knobs to improve the performance during extensive simulations. For the results presented in the next subsection, these performance matrices were chosen to be independent of k and α_{0i}.

The resulting finite set of synthesized controller coefficients, for example $\{A_k^c(\bar{\alpha}_{0i})\}$, were interpolated using least squares fitting yielding a family of continuously parameter dependent controllers, corresponding to (21), whose describing matrices are quadratically parameter dependent, for example

$$A_k^c(\alpha_0) = A_k^{c1} + \alpha_0 A_k^{c2} + \alpha_0^2 A_k^{c3}$$

The disadvantage of this technique is that by the interpolation process there is no guarantees that, even for fixed parameter values, the controller obtained by interpolation stabilizes the closed loop system. An a posteriori analysis showed that for a dense grid of fixed values of α_0 the closed loop system is stabilized. In this particular case, this would not happen if we had used a simpler linear interpolation instead of a quadratic interpolation. Note also that using a piecewise linear interpolation would not comply with the assumption that the scheduling controller is a continuously differentiable function of the scheduling variable.

Having designed the family of controllers $C(\alpha_0)$, the non-linear controller $K(\alpha_k)$ can be implemented as in (23), where $\alpha_k = \gamma_k$ becomes a time-varying parameter computed according to (28). The final implementation scheme is shown in Figure 5. Notice that system C_I in this particular case degenerates into simple integrators $C_I = \frac{1}{1-z^{-1}}I_4$ since the actuators were considered synchronous and updated at a sampling rate of 50 Hz.

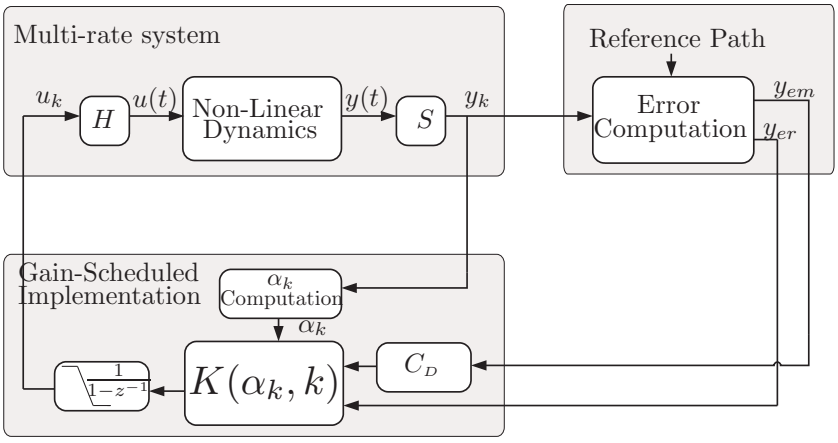

Figure 5. Block diagram with the final implementation scheme

Some additional features of this implementation are worthwhile emphasizing. The placement of the integrators at the plant's input, has the following advantages: *i)* the implementation of anti-windup schemes is straightforward *ii)* auto-trimming property- the controller automatically generates adequate trimming values for the actuation signals. Though in the present case simple integrators are being used, the same advantages would hold if the inputs were updated at different rates and the integrators took the form of Ω_I, (14).

5.5. Simulation Results

We start with a simple example that compares the performance of a multi-rate guidance and control law with that obtained using a standard single-rate $\mathcal{H}_2$ compensator designed using equivalent weighting matrices. First, we compare the values of the closed-loop $\mathcal{H}_2$ norms while changing the rate of the linear position measurement and keeping the sampling periods of the other outputs and of the input at $t_s = 0.02$ s. The periodic $\mathcal{H}_2$ controllers were synthesized for a single operating condition, characterized by $\xi_0 = \begin{bmatrix} V_C & \gamma_C & \dot{\psi}_C & \psi_{CT} \end{bmatrix}^T = \begin{bmatrix} 1\,\mathrm{m.s^{-1}} & 0\,\mathrm{rad} & 0\,\mathrm{rad.s^{-1}} & 0\ \mathrm{rad} \end{bmatrix}^T$. The results are shown in Table I.

Notice that when the sampling rate of the linear position measurement equals the sampling rate of the other outputs ($t_s = 0.02$ s), the multi-rate set-up particularizes to the single-rate case and the periodic $\mathcal{H}_2$ controller is equivalent to a standard discrete-time $\mathcal{H}_2$ controller. As expected the performance of the closed-loop system, given in terms of the $\mathcal{H}_2$ norm, deteriorates as the sampling period for the linear position increases. In order to assess the impact of this performance loss on the tracking response of the vehicle, a simple maneuver task is set up for the rotorcraft. During the maneuver the vehicle is required to follow a path with constant velocity $V_C = 1\ \mathrm{m.s^{-1}}$ and constant orientation with respect to the path, consisting of: *i)* a level flight segment along the x axis, *ii)* a climbing ramp with a flight path angle of $\gamma_C = \frac{\pi}{6}$ rad, *iii)* a level flight segment along the x axis. A gain-scheduled controller was synthesized following the procedure given in Section 5.5.4 for constant parameters $\varphi_0 = (V_C, \dot{\psi}_C, \psi_{CT}) = (1\,\mathrm{m.s^{-1}}, 0\,\mathrm{rad.s^{-1}}, 0\,\mathrm{rad})$. For the single-rate case, all the outputs are measured at a sampling rate of $t_s = 0.02$ s, and for the multi-rate case, the sampling rates are given according to Section 5.5.3. The results comparing these two cases, which include the temporal evolution of the actuation, dynamic variables v and ω, and kinematic errors $p_E = p_B - p_C = [x_E \ \ y_E \ \ z_E]^T$ and $\lambda_E = \lambda_B - \lambda_C = [\phi_E \ \ \theta_E \ \ \psi_E]^T$, are shown in Figures 6 and 7.

As expected, we can notice some degradation in the actuation and error responses for the multi-rate case in comparison with the single-rate case. Nevertheless, while the proposed method takes into account the multi-rate characteristics of the sensors, it also achieves good tracking performance and displays a smooth behavior throughout the different stages of the trajectory. Notice also that, as desired, steady-state is achieved after the transitions between trimming trajectories, with zero-steady state value for $y_{er} = [p_e \ \ \psi_e]$, and that the trimming values for the actuation are naturally acquired.

Another simulation is presented in order to test the proposed methodology in other flight conditions as well as analyze the impact of noise in the sensors. In this simulation the vehicle is required to follow a path with constant velocity $V_C = 5\mathrm{m.s^{-1}}$ and constant orientation with respect to the path, consisting of *i)* a level flight segment along the x axis, *ii)* a climbing helix with a flight path angle of $\gamma_C = 0.29$ rad and yaw rate $\dot{\psi}_C = 0.26\ \mathrm{rad.s^{-1}}$, *iii)* a level flight segment along the x axis. The controller is synthesized according to the

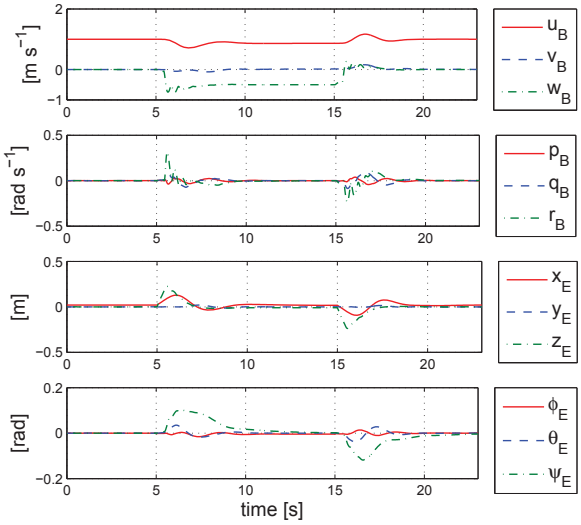

(a) Errors multi-rate

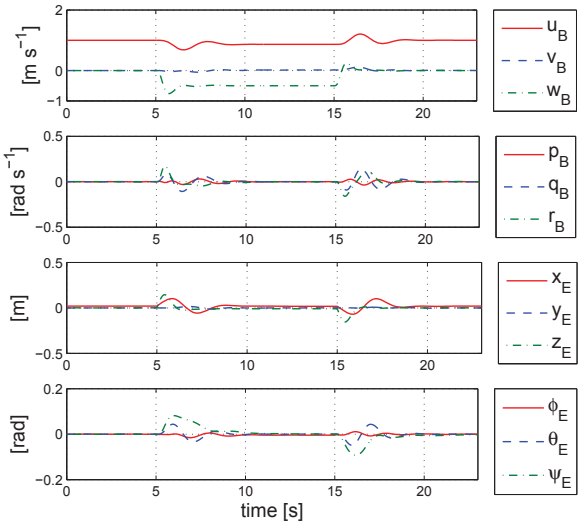

(b) Errors single-rate

Figure 6. Results for the first simulation- Errors

methodology presented in Section 5.5.4 for constant parameters $\varphi_0 = (V_C, \dot{\psi}_C, \psi_{CT}) = (5\,\mathrm{m.s}^{-1}, 0\,\mathrm{rad.s}^{-1}, 0\,\mathrm{rad})$ and the weights of the $\mathcal{H}_2$ controller synthesis problem, described in (32) are changed to accommodate for the different operating conditions. We have

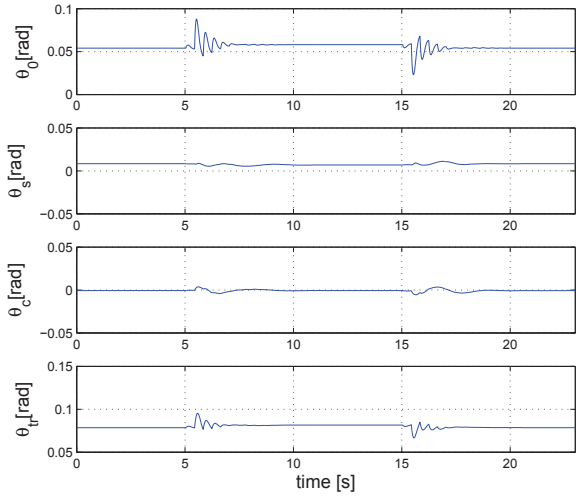

(a) Actuation multi-rate

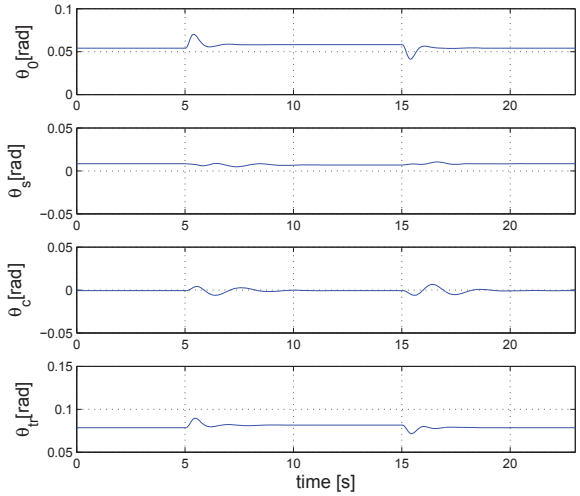

(b) Actuation single-rate

Figure 7. Results for the first simulation- Actuation

considered additive white gaussion noise for all the measurements with autocorrelations matrices $(R_{vv}(\tau), R_{\omega\omega}(\tau), R_{pp}(\tau), R_{\lambda\lambda}(\tau) = (\sigma_v^2 I\delta(\tau), \sigma_\omega^2 I\delta(\tau), \sigma_p^2 I\delta(\tau), \sigma_\lambda^2 I\delta(\tau))$, where $(\sigma_v, \sigma_\omega, \sigma_p, \sigma_\lambda) = (0.02\ \mathrm{m.s}^{-1}, 0.3^o.\mathrm{s}^{-1}, 0.1\ \mathrm{m}, 0.5^o)$. The results presented in Figure 8 show that good sensor noise rejection is achieved and that the helicopter performs the required task keeping the actuation within the limits of operation. A 3-D view of both maneuvers is shown

in Figure 9.

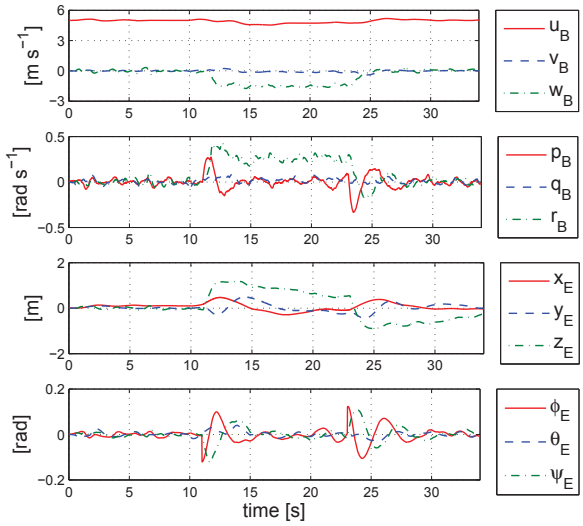

(a) Errors

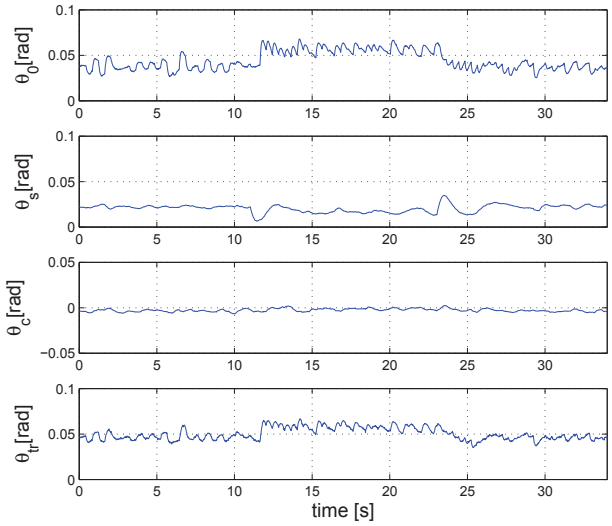

(b) Actuation

Figure 8. Results for the second simulation

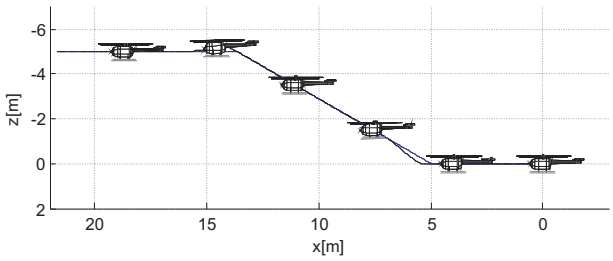

(a) First Simulation

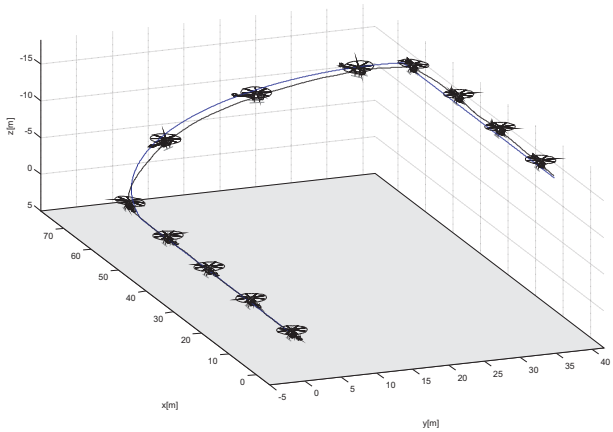

(b) Second Simulation

Figure 9. Rotorcraft Maneuvers

6. CONCLUSIONS

A new method was proposed for the design and implementation of gain-scheduled controllers for multi-rate systems with application on the field of integrated guidance and control for autonomous vehicles. In contrast to previous approaches, where the multi-rate characteristics of the sensors are handled by the navigation system, this approach provides an alternative framework that directly takes into account these characteristics in the control system.

A theoretical formulation was presented to tackle the problem of designing and implementing gain-scheduled controllers for non-square multi-rate systems. The formulation is valid for a wide class of non-linear plants and its application to other control problems is an interesting topic for future work.

The proposed technique was applied to provide a solution to the design of integrated guidance and control systems that address the trajectory tracking problem for small-scale rotorcraft. Simulation results illustrate the effectiveness of the controller along simple maneuvers when the vehicle linear position is measured at a lower rate than that of the remaining state variables.

Appendix

Proof 6. *(of Theorem 1) The system G_a described by* (17)*, can be seen as the series connection of two systems $G_a = G_{a2}G_{a1}$, where*

$$G_{a1} = \begin{cases} x_{k+1} = Fx_k + G\Omega_k u_k \\ y_k = \begin{bmatrix} y_{mk} \\ y_{rk} \end{bmatrix} = \Gamma_k \begin{bmatrix} H_m \\ H_r \end{bmatrix} x_k = \begin{bmatrix} \Gamma_{mk} & 0 \\ 0 & \Gamma_{rk} \end{bmatrix} \begin{bmatrix} H_m \\ H_r \end{bmatrix} x_k \end{cases}, \tag{34}$$

$$F = \begin{bmatrix} A_d & B_d \\ 0 & I \end{bmatrix}, \quad G = \begin{bmatrix} B_d \\ I \end{bmatrix}, \quad H_m = \begin{bmatrix} C_{dm} & 0 \end{bmatrix}, \quad H_r = \begin{bmatrix} C_{dr} & 0 \end{bmatrix}, \tag{35}$$

and

$$G_{a2} = \begin{cases} x^D_{k+1} = (I - \Gamma_{mk})x^D_k + \begin{bmatrix} \Gamma_{mk} & 0 \end{bmatrix} u^D_k \\ y^D_k = -\begin{bmatrix} \Gamma_{mk} \\ 0 \end{bmatrix} x^D_k + \begin{bmatrix} \Gamma_{mk} & 0 \\ 0 & \Gamma_{rk} \end{bmatrix} u^D_k \end{cases}.$$

By Lemma 1 it suffices to establish that the lift $\bar{G}_a$ of system G_a is detectable and stabilizable. This LTI sytem $\bar{G}_a$ can be determined by computing separately the lifts of G_{a1} and G_{a2} and using the fact that the lift of the series of two systems is the series of the lifts of each one, i.e., $\bar{G}_a = \bar{G}_{a2}\bar{G}_{a1}$. For simplicity, we restrict u, y_r and y_m to be 1-dimensional signals, i.e. $u, y_r, y_m \in l(\mathbb{Z}^+, \mathbb{R})$. The proof for the general case follows the same ideas but the algebra is more cumbersome.

Let P be a permutation matrix such that

$$\overline{\begin{bmatrix} y_{ml} \\ y_{rl} \end{bmatrix}} = P \begin{bmatrix} \bar{y}_{ml} \\ \bar{y}_{rl} \end{bmatrix}$$

where $\overline{\begin{bmatrix} y_{m\,l} \\ y_{r\,l} \end{bmatrix}} = \begin{bmatrix} y_{m\,l} & y_{r\,l} & y_{m\,l+1} & y_{r\,l+1} & \cdots & y_{m\,l+h-1} & y_{r\,l+h-1} \end{bmatrix}^T$,
$\bar{y}_{m\,l} = \begin{bmatrix} y_{m\,l} & y_{m\,l+1} & \cdots & y_{m\,l+h-1} \end{bmatrix}^T$ *and* $\bar{y}_r = \begin{bmatrix} y_{r\,l} & y_{r\,l+1} & \cdots & y_{r\,l+h-1} \end{bmatrix}^T$*, and define the matrices*

$$\bar{H}_m = \begin{bmatrix} H_m \\ H_m F \\ \vdots \\ H_m F^{h-1} \end{bmatrix} \quad \bar{H}_r = \begin{bmatrix} H_r \\ H_r F \\ \vdots \\ H_r F^{h-1} \end{bmatrix} \tag{36}$$

$$\bar{D}_m = \begin{bmatrix} 0 & \cdots & \cdots & \cdots & 0 \\ H_m G & 0 & \cdots & \cdots & 0 \\ H_m FG & H_m G & 0 & \cdots & 0 \\ \vdots & \vdots & \vdots & \ddots & 0 \\ H_m F^{h-2} G & H_m F^{h-3} G & \cdots & H_m G & 0 \end{bmatrix} \quad \bar{D}_r = \begin{bmatrix} 0 & \cdots & \cdots & \cdots & 0 \\ H_r G & 0 & \cdots & \cdots & 0 \\ H_r FG & H_r G & 0 & \cdots & 0 \\ \vdots & \vdots & \vdots & \ddots & 0 \\ H_r F^{h-2} G & H_r F^{h-3} G & \cdots & H_r G & 0 \end{bmatrix}.$$

Then, the lift of system G_{a1} is given by

$$\bar{G}_{a1} = \begin{cases} \bar{x}_{l+1} = \bar{F}\bar{x}_l + \bar{G}\bar{\Omega}\bar{u}_l \\ \bar{y}_l = P\left(\begin{bmatrix} \bar{\Gamma}_m & 0 \\ 0 & \bar{\Gamma}_r \end{bmatrix} \begin{bmatrix} \bar{H}_m \\ \bar{H}_r \end{bmatrix} \bar{x}_l + \begin{bmatrix} \bar{\Gamma}_m & 0 \\ 0 & \bar{\Gamma}_r \end{bmatrix} \begin{bmatrix} \bar{D}_m \\ \bar{D}_r \end{bmatrix} \bar{\Omega}\bar{u}_l \right) \end{cases}.$$

where $\bar{F}$ *and* $\bar{G}$ *are defined as in* (13)*, and* $\bar{\Gamma}_m$ *and* $\bar{\Gamma}_r$ *are defined as in* (6)*. Defining the matrices*

$$\bar{B}_l = \begin{bmatrix} 0 & \dots & 0 & 1 \end{bmatrix} \Pi_{\Gamma_m} \quad \bar{C}_l = \Pi_{\Gamma_m}^T \begin{bmatrix} -1 \\ 0 \\ \dots \\ 0 \end{bmatrix} \quad \bar{D}_l = \Pi_{\Gamma_m}^T \begin{bmatrix} 1 & 0 & 0 & \dots & 0 \\ -1 & 1 & 0 & \dots & 0 \\ \vdots & \ddots & \ddots & \ddots & 0 \\ 0 & 0 & \dots & -1 & 1 \end{bmatrix} \Pi_{\Gamma_m} \tag{37}$$

where Π_{Γ_m}, Π_{Γ_r} *are the projection matrices defined at the end of Subsection (2.2.2), we can show that the lift of system* G_{a2} *is described by*

$$\bar{G}_{a2} = \begin{cases} \bar{x}_{l+1}^D = \begin{bmatrix} \bar{B}_l & 0 \end{bmatrix} \begin{bmatrix} \bar{\Gamma}_m & 0 \\ 0 & \bar{\Gamma}_r \end{bmatrix} P^{-1} \bar{u}_l^D \\ \bar{y}_{l+1}^D = P \begin{bmatrix} \bar{\Gamma}_m \bar{C}_l \\ 0 \end{bmatrix} \bar{x}_l^D + P \begin{bmatrix} \bar{\Gamma}_m \bar{D}_l \bar{\Gamma}_m & 0 \\ 0 & \bar{\Gamma}_r \end{bmatrix} P^{-1} \bar{u}_l^D \end{cases}$$

Computing the series of $\bar{G}_{a1}$ *and* $\bar{G}_{a2}$ *yields*

$$\bar{G}_a = \begin{cases} \begin{bmatrix} \bar{x}_{l+1} \\ \bar{x}_{l+1}^D \end{bmatrix} = \bar{M} \begin{bmatrix} \bar{x}_l \\ \bar{x}_l^D \end{bmatrix} + \bar{N} \bar{u}_l \\ \bar{y}_l^D = \bar{K} \begin{bmatrix} \bar{x}_l \\ \bar{x}_l^D \end{bmatrix} + \bar{L} \bar{u}_l \end{cases}$$

where

$$\begin{aligned} \bar{M} &= \begin{bmatrix} \bar{F} & 0 \\ \bar{B}_l \bar{\Gamma}_m \bar{H}_m & 0 \end{bmatrix}, \quad \bar{N} = \begin{bmatrix} \bar{G} \\ \bar{B}_l \bar{\Gamma}_m \bar{D}_m \end{bmatrix} \bar{\Omega}, \\ \bar{K} &= P \begin{bmatrix} \Pi_{\Gamma_m}^T & 0 \\ 0 & \Pi_{\Gamma_r}^T \end{bmatrix} \begin{bmatrix} \Pi_{\Gamma_m} \bar{D}_l \bar{\Gamma}_m \bar{H}_m & \Pi_{\Gamma_m} \bar{C}_l \\ \Pi_{\Gamma_r} \bar{H}_r & 0 \end{bmatrix} \text{ and} \\ \bar{L} &= P \begin{bmatrix} \Pi_{\Gamma_m}^T & 0 \\ 0 & \Pi_{\Gamma_r}^T \end{bmatrix} \begin{bmatrix} \Pi_{\Gamma_m} \bar{D}_l \bar{\Gamma}_m & 0 \\ 0 & \Pi_{\Gamma_r} \end{bmatrix} \begin{bmatrix} \bar{D}_m \\ \bar{D}_r \end{bmatrix} \bar{\Omega} \end{aligned}$$

To establish detectability of the pair $(\bar{M}, \bar{K})$ *and stabilizability of the pair*$(\bar{M}, \bar{N})$*, we start by determining the unstable eigenvalues* $\Lambda = \{\lambda : \lambda \text{ is eigenvalue of } \bar{M} \text{ and } \|\lambda\| \geq 1\}$ *and corresponding left and right eigenvector* $P = \{p : \bar{M}p = \lambda p, \lambda \in \Lambda\}$ *and* $Q = \{q : q^T \bar{M} = \lambda q^T, \lambda \in \Lambda\}$*, respectively. From the structure of* $\bar{M}$*,* Λ *coincides with the unstable eigenvalues of* $\bar{F}$ *and* P *and* Q *can be written as,* $P = \{p : p = [v^T \ ((\bar{B}_l \bar{\Gamma}_m \frac{\bar{H}_m}{\lambda})v)^T]^T, \ \ \bar{F}v = \lambda v, \ \ \lambda \in \Lambda\}$ *and* $Q = \{q : q^T = [w^T \ 0], \ \ w^T \bar{F} = \lambda w^T, \ \ \lambda \in \Lambda\}$*, respectively. As stated in [5], assumption iii) implies that* v *is an eigenvector of* F *associated with an unstable eigenvalue* μ *if and only if it is an eigenvector of* $\bar{F}$ *associated with* $\lambda = \mu^h$*, i.e.,*

$$Fv = \mu v \Leftrightarrow \bar{F}v = \mu^h v \quad \text{and} \quad w^T F = \mu w^T \Leftrightarrow w^T \bar{F} = \mu^h w^T.$$

Taking into account the structure of F *defined in* (35)*, we can partition the unstable eigenvalues of* $\bar{M}$ *into* $\Lambda = \Lambda_A \cup \Lambda_I$*, where* Λ_I *are* m *unitary eigenvalues and*

$$\Lambda_A = \{\lambda : \lambda = \mu^h, \mu \text{ is an eigenvalue of } A_d \text{ and } \|\mu\| \geq 1\}$$

and partition accordingly the associated eigenvectors, $P = P_A \cup P_I$ and $Q = Q_A \cup Q_I$, where

$$P_A = \{p : p = [v^T \;\; ((\bar{B}_l\bar{\Gamma}_m\frac{\bar{H}_m}{\mu^h})v)^T]^T, \quad v = [v_a^T \;\; 0]^T, \quad A_d v_a = \mu v_a \quad \mu^h \in \Lambda\}$$

$$P_I = \{p : p = [v^T \;\; ((\bar{B}_l\bar{\Gamma}_m\frac{\bar{H}_m}{\mu^h})v)^T]^T, \quad v = [v_a^T \;\; v_b^T]^T, \quad [A_d - I \;\; B_d]\,[v_a^T \;\; v_b^T]^T = 0\}$$

$$Q_A = \{q : q^T = [w^T \;\; 0], w^T = [w_a^T \;\; \frac{w_a^T B_d}{\mu - 1}] \;\; w_a^T A_d = \mu w_a^T, \quad \mu^h \in \Lambda\}$$

$$Q_I = \{q : q^T = [w^T \;\; 0]^T, w^T = [0 \;\; w_b^T], \quad w_b \in \mathbb{R}^m \backslash \{0\}\}.$$

Notice that Q_A is well-defined since by assumption iii) $\mu \neq 1$. We are then in conditions to apply the standard PHB test to prove stabilizability and detectability of $\bar{G}_a$, i.e. $q^T\bar{M} = \lambda q^T \implies q^T\bar{N} \neq 0$, and $\bar{M}p = \lambda p \implies \bar{K}p \neq 0$, respectively.

Stabilizability

For $q^T = [w^T \;\; 0] = [[w_a^T \;\; \frac{w_a^T B_d}{\mu-1}] \;\; 0] \in Q_A$, $w_a^T A_d = \mu w_a^T$ we have

$$q^T\bar{N} = w^T\bar{G}\bar{\Omega} = (1 + \frac{1}{\mu - 1})\left[\mu^{h-1}w_a^T B_d\Omega_0 \quad \mu^{h-2}w_a^T B_d\Omega_1 \quad \dots \quad w_a^T B_d\Omega_{h-1}\right] \neq 0$$

where we used assumption i) ($w_a^T B_d \neq 0$) and assumption ii).
For $q^T = [w^T \;\; 0] = [[0 \;\; w_b^T] \;\; 0] \in Q_I$

$$q^T\bar{N} = w^T\bar{G}\bar{\Omega} = \left[w_b^T\Omega_0 \quad \dots \quad w_b^T\Omega_{h-1}\right] \neq 0$$

by assumption ii).

Detectability

For $p = [v^T \;\; ((\bar{B}_l\bar{\Gamma}_m\frac{\bar{H}_m}{\mu^h})v)^T]^T \in P_A$, $v = [v_a^T \;\; 0]^T \;\; A_d v_a = \mu v_a$ we have

$$\bar{K}p = P\begin{bmatrix}\Pi_{\Gamma_m}^T & 0\\ 0 & \Pi_{\Gamma_r}^T\end{bmatrix}\begin{bmatrix}\Pi_{\Gamma_m}\bar{D}_l\bar{\Gamma}_m\bar{H}_m & \Pi_{\Gamma_m}\bar{C}_l\\ \Pi_{\Gamma_r}\bar{H}_r & 0\end{bmatrix}\begin{bmatrix}v\\ (\bar{B}_l\bar{\Gamma}_m\frac{\bar{H}_m}{\mu^h})v\end{bmatrix}$$

and thus it suffices to prove that

$$\begin{bmatrix}\Pi_{\Gamma_m}\bar{D}_l\bar{\Gamma}_m\bar{H}_m & \Pi_{\Gamma_m}\bar{C}_l\\ \Pi_{\Gamma_r}\bar{H}_r & 0\end{bmatrix}\begin{bmatrix}v\\ (\bar{B}_l\bar{\Gamma}_m\frac{\bar{H}_m}{\mu^h})v\end{bmatrix} \neq 0. \tag{38}$$

From the definitions of $\bar{H}_m$, $\bar{B}_l$, $\bar{C}_l$ and $\bar{D}_l$ and from assumption ii) it is easy to see that $\bar{B}_l\bar{\Gamma}_m\bar{H}_m v = \mu^i\,[C_{dm} \;\; 0]\,v$ for some $i \in \{0, ..., h-1\}$, and that

$$\begin{bmatrix}\Pi_{\Gamma_m}\bar{D}_l\bar{\Gamma}_m\bar{H}_m & \Pi_{\Gamma_m}\bar{C}_l\\ \Pi_{\Gamma_r}\bar{H}_r & 0\end{bmatrix} = \left[\begin{array}{cc}\begin{bmatrix}1 & 0 & 0 & \dots & 0\\ -1 & 1 & 0 & \dots & 0\\ \vdots & \ddots & \ddots & \ddots & 0\\ 0 & 0 & \dots & -1 & 1\end{bmatrix}\Pi_{\Gamma_m}\bar{H}_m & \begin{bmatrix}-1\\ 0\\ \vdots\\ 0\end{bmatrix}\\ \multicolumn{2}{c}{\Pi_{\Gamma_r}\bar{H}_r \qquad\qquad 0}\end{array}\right] \tag{39}$$

One can also verify that

$$[1\ \ 0\ \ \ldots\ \ 0]\,\Pi_{\Gamma_m}\bar{H}_m v = [C_{dm}\ \ 0]\,\mu^j v \ \text{ for some } \ j \in \{0, ..., h-1\}$$

and

$$[1\ \ 0\ \ \ldots\ \ 0]\,\Pi_{\Gamma_r}\bar{H}_r v = [C_{dr}\ \ 0]\,\mu^k v \ \text{ for some } \ k \in \{0, ..., h-1\}$$

from which two of the lines of the left-hand side of (38) *are given by*

$$\begin{bmatrix} (C_{dm}\mu^j - C_{dm}\frac{1}{\mu^{h-i}}) & 0 \\ C_{dr}\mu^k & 0 \end{bmatrix} v = \begin{bmatrix} (\mu^j - \frac{1}{\mu^{h-i}}) & 0 \\ 0 & \mu^k \end{bmatrix} C_d v_a.$$

This establishes (38)*, since by assumption iii)* $\mu \neq 1$ *and by assumption i)* $C_d v_a \neq 0$*.*

For $p = [v^T\ \ ((\bar{B}_l\bar{\Gamma}_m\frac{\bar{H}_m}{\mu^h})v)^T]^T \in P_I$*,* $[A_d - I\ \ B_d]v = 0$*, it can be verified that the first rows of* (38) *are zero* $\Pi_{\Gamma_m}\bar{D}_l\bar{\Gamma}_m\bar{H}_m v + \Pi_{\Gamma_m}\bar{C}_l(\bar{B}_l\bar{\Gamma}_m\frac{\bar{H}_m}{\mu^h})v = 0$*. However, the last rows are different from zero* $\Pi_{\Gamma_r}\bar{H}_r v \neq 0$*, since otherwise the condition* $\Pi_{\Gamma_r}\bar{H}_r v = 0$ *would imply* $[C_{dr}\ \ 0]\,v = 0$ *and we would have* $\begin{bmatrix} A_d - I & B_d \\ C_{dr} & 0 \end{bmatrix} v = 0$ *which contradicts assumption iv) of the theorem.*

Proof 7. *(of Lemma 3) Suppose that the expression for the controller* C_K *that asymptotically stabilizes* (17) *is given by*

$$C_K = \left\{ \begin{bmatrix} x_{k+1}^K \\ y_k^C \end{bmatrix} = \begin{bmatrix} A_k^K & B_k^K \\ C_k^K & D_k^K \end{bmatrix} \begin{bmatrix} x_k^K \\ y_k^A \end{bmatrix} \right.$$

It is straightforward to check that the equilibrium values for the feedback connection of C_K *and* G_a *are*

$$\underline{x}^K = 0 \ \ , \ \ \underline{y}^C = 0 \ \ , \ \ \underline{y}^A = 0,$$

$$\underline{x} = x_0 \ \ , \ \ \underline{x}^I = u_0 \ \ , \ \ \underline{x}^D = y_{m0}$$

and that these values yield the steady-state value $y_0 = C_r x_0 = r_0$ *for* y_r*. Due to linearity and asymptotic stability the system trajectories will tend to this unique equilibrium point even in the presence of disturbances that do not affect asymptotic stability.*

REFERENCES

1. S. Bittanti and P. Bolzern. Stabilizability and detectability of linear periodic systems. *System & Control Letters*, 6(2):141–146, 1985.
2. S. Bittanti, P. Colaneri, and G. Nicolao. The difference periodic riccati equation for the periodic prediction problem. *IEEE Transactions on Automatic Control*, 33(8):706–712, August 1988.
3. P. Colaneri. Output stabilization via pole placement of discrete-time linear periodic systems. *IEEE Transactions on Automatic Control*, 36(6):739–742, June 1991.
4. P. Colaneri and G. Nicolao. Multirate lqg control of continuous-time stochastic systems. *Automatica*, 31(4):591–596, April 1995.
5. P. Colaneri, R. Scattolini, and N. Schiavoni. Regulation of multirate sampled-data systems. *Control-Theory and Advanced Technology*, 7(3):429–441, 1991.
6. R. Cunha, D. Antunes, and C. Gomes, P. Silvestre. A path-following preview controller for autonomous air vehicles. In *AIAA Guidance, Navigation, and Control Conference*, Keystone, August 2006. AIAA.

7. R. Cunha and C. Silvestre. Dynamic modeling and stability analysis of model-scale helicopters with bell-hiller stabilizing bar. In *AIAA Guidance, Navigation, and Control Conference*, Austin, TX, August 2003. AIAA.
8. B. Francis and W. M. Wonham. The internal model principle of control theory. *Automatica*, 12:457–465, September 1976.
9. I. Kaminer, A. Pascoal, E. Hallberg, and C. Silvestre. Trajectory tracking for autonomous vehicles: An integrated approach to guidance and control. *AIAA Journal of Guidance, Control, and Dynamics*, 21(1):29–38, 1998.
10. I. Kaminer, A. Pascoal, P. Khargonekar, and E. Coleman. A velocity algorithm for the implementation of gain-scheduled controllers. Technical report, Naval Postgraduate School, 1994.
11. I. Kaminer, A. Pascoal, P. Khargonekar, and E. Coleman. A velocity algorithm for the implementation of gain-scheduled controllers. *Automatica*, 31(8):1185–1191, August 1995.
12. Hassan Khalil. *Nonlinear Systems, Third Edition*. Prentice Hall, Upper Saddle River, NJ, 2000.
13. S. Lall and G. Dullerud. An lmi solution to the robust synthesis problem for multi-rate sampled-data systems. *Automatica*, 37, 2001.
14. P. Oliveira and A. Pascoal. On the design of multirate complementary filters for autonomous marine vehicle navigation. In *GCUV2003 - 1st IFAC Workshop on Guidance and Control of Underwater Vehicles*, Newport, UK, 2003.
15. H. Rahmani and G. Franklin. A new optimal multirate control of linear periodic and time-invariant systems. *IEEE Transactions on Automatic Control*, 35(4):406–415, April 1990.
16. W. Rugh and J. Shamma. Research on gain scheduling. *Automatica*, 36:1401–1425, October 2000.
17. C. Silvestre, A. Pascoal, and I. Kaminer. On the design of gain-scheduled trajectory tracking controllers. *International Journal of Robust and Nonlinear Control*, 12:797–839, 2002.
18. B. Stevens and F. Lewis. *Aircraft Control and Simulation*. John Wiley & Sons, New York, USA, 1992.
19. J. Stoustrup Wisniewski R. Periodic h_2 synthesis for spacecraft attitude control with magnetometers. *AIAA Journal of Guidance, Control, and Dynamics*, 27(5):874–881, 2004.

Table I. $\mathcal{H}_2$ closed-loop values for different position sampling rates

Linear position sampling period t_{sp}(s)	0.02	0.04	0.1	0.2	0.4
Closed loop $\mathcal{H}_2$ norm $\|G_{cl}\|_2$	10.40	11.08	12.18	13.15	14.27